© 2017. Published by The Company of Biologists Ltd | Journal of Experimental Biology (2017) 220, 517-530 doi:10.1242/jeb.134056

REVIEW

Mussel adhesion – essential footwork

J. Herbert Waite*

ABSTRACT

Robust adhesion to wet, salt-encrusted, corroded and slimy surfaces has been an essential adaptation in the life histories of sessile marine organisms for hundreds of millions of years, but it remains a major impasse for technology. Mussel adhesion has served as one of many model systems providing a fundamental understanding of what is required for attachment to wet surfaces. Most polymer engineers have focused on the use of 3,4-dihydroxyphenyl-L-alanine (Dopa), a peculiar but abundant catecholic amino acid in mussel adhesive proteins. The premise of this Review is that although Dopa does have the potential for diverse cohesive and adhesive interactions, these will be difficult to achieve in synthetic homologs without a deeper knowledge of mussel biology; that is, how, at different length and time scales, mussels regulate the reactivity of their adhesive proteins. To deposit adhesive proteins onto target surfaces, the mussel foot creates an insulated reaction chamber with extreme reaction conditions such as low pH, low ionic strength and high reducing poise. These conditions enable adhesive proteins to undergo controlled fluid–fluid phase separation, surface adsorption and spreading, microstructure formation and, finally, solidification.

KEY WORDS: Dopa, Foot behavior, Interfacial chemistry, Mussel foot proteins

Introduction

Wind- and wave-swept seashores are home to countless sessile organisms that spend part or most of their lives attached to surfaces by way of holdfasts. Besides the established importance of holdfasts for organism development and survival (Yonge, 1962; Denny and Gaylord, 2010), holdfasts are also crucial for mariculture (Hurlburt and Hurlburt, 1975), as sentinels of contamination (Koide et al., 1982) and climate change (O'Donnell et al., 2013), as scaffolds for reef-like ecosystems (Witman, 1987), as mediators of marine fouling (Ricciardi, 1998), and as model systems for mimicking opportunistic wet adhesion (Lee et al., 2011). The last-mentioned has been the primary focus of research in my group and has considerable translational appeal to biomedical and industrial adhesive technologies, because the presence of moisture, salts, corrosion and films on surfaces subverts most known synthetic adhesives.

The byssus-mediated adhesion of clustered and individual mussels is probably the best studied and most emulated of marine holdfasts (Fig. 1A). The byssus consists of a bundle of threads, each 2–6 cm in length in an adult mussel, and contains three parts: a spatulate adhesive plaque, a stiff distal portion and a compliant proximal portion. Byssal threads probably evolved from extracellular matrix; protein domains resembling collagen (Harrington and Waite, 2007), integrins (Suhre et al., 2014) and epidermal growth factor (Hwang et al., 2010a) are abundant in byssal proteins. Emulation has been largely limited to adapting Dopa (3,4-dihydroxyphenyl-L-alanine), a catecholic amino acid in mussel adhesive proteins, for a variety of synthetic polymers. Dopa also occurs in the cement of sandcastle worms and tunicates, among others (Taylor et al., 1997; Waite et al., 1992). The reluctance of biotechnology to mimic anything but Dopa is unfortunate, because mussels offer profound insights at multiple length scales and time scales for implementing wet adhesion; even the successful translation of Dopa for adhesion technology depends on a deeper understanding of how mussels regulate the chemistry of catechols (see Glossary). Thus, the theme of this Review is to correct the widespread misconception that mussel adhesion depends on a single molecular entity; instead, it owes its performance to the coordination of critical processing details, including protein fabrication and phase behavior, and delivery, deposition, assembly and curing of components. Indeed, mussel adhesion is as reliant on processing history as are the best-performing industrial adhesives (Wake, 1982).

Marine Sciences Institute, University of California–Santa Barbara, Santa Barbara, CA 93106, USA.

*Author for correspondence (waite@lifesci.ucsb.edu)

J.H.W., 0000-0003-4683-7386

The mussel foot: versatile adhesive fabricator and applicator

Every byssal thread and plaque has two stages of development: the first is a short-lived, nonfunctional nascent stage, during which various molecular components are assembled in and under the foot. The second is a long-lived stage that begins after the foot disengages from the thread, which is recruited into load-bearing service. Here, I review the role of the foot in the production of a new byssal thread in members of the genus *Mytilus*, particularly *Mytilus edulis* Linnaeus 1758, *Mytilus galloprovincialis* Lamarck 1819 and *Mytilus californianus* Conrad 1837 (Fig. 1A).

Anatomy of the mussel foot and adhesive production sites

The mussel foot (Fig. 1B) has remarkable synthetic, tactile and building activities, and produces the entire byssus, one thread at a time, in its ventral groove (Waite, 1992) (Fig. 1C). Fabrication of byssal threads takes 30 seconds to 8 minutes per thread, depending on mussel age, with juvenile mussels being fastest (Martinez Rodriguez et al., 2015). Thread formation is reminiscent of controlled delivery by a microfluidic device: three major gland reservoirs – the phenol, collagen and accessory glands – feed specific amounts of their contents into the ventral groove, around which they are organized (Tamarin and Keller, 1972; Vitellaro Zuccarello, 1980) (Fig. 1C; Table 1). These glands are responsible for the synthesis and storage of the molecular components of the adhesive plaque, the collagenous thread core and the cuticle – a biological varnish. Consistent with protein synthesis, the glands contain an extensive endoplasmic reticulum studded with ribosomes, and a number of membrane-bound inclusion granules with ultrastructures specific to each gland type (Tamarin et al., 1972). In response to poorly understood signals, rows of granules migrate through narrow elongations of cytoplasm before releasing their contents into conducting tubules that connect with the ventral groove or distal

Journal of Experimental Biology (2017) 220, 517-530 doi:10.1242/jeb.134056

Glossary

Catechol
A family of organic compounds containing o-dihydroxybenzene. Dopa is essentially a catechol joined with the amino acid alanine.

Cation-π interaction
An electrostatic interaction between a cation such as K^+ or the ε-amino group of lysine and the electron-rich π face of an aromatic ring (Dougherty, 2013).

Chemisorption
Adsorption to a surface by chemical, e.g. covalent bonds, as opposed to the noncovalent bonds involved in physisorption.

Condensation
Occurs when dilute oppositely charged polyelectrolytes in solution combine by electrically neutralizing one another to form coacervate microdroplets of concentrated, partially dehydrated polyelectrolytes.

Coordination bond
A molecular interaction between an electron donor (Lewis base) and electron acceptor (Lewis acid) where the donor is rich in nonbonding electron pairs (e.g. imidazole and catechol) and the acceptor is a transition metal ion with unfilled d-orbitals. Unlike the electron sharing between two atoms in a covalent bond, in a coordination bond the ligand provides all the electrons whereas the metal merely accommodates the electrons. The coordination bond is nearly as strong as a covalent bond but, unlike the latter, reforms after breakage, and thus offers profound opportunities for self-healing materials.

Debye screening
According to Debye–Hückel theory, an ion has an electrical sphere of influence that is specified by its Debye radius. The radius is inversely proportional to the surrounding dielectric constant and salt concentration. The saltier the water, the closer two ions have to get before any repulsion or attraction is felt. In effect, high salinity screens the two ions from one another.

Dielectric constant (ε)
A polarization property of different media. In an electric field, water and formamide are highly polarized, whereas vacuum and nonpolar solvents are not. High ε media weaken most noncovalent interactions. In Coulomb's law, for example, the electrostatic interaction energy E between two oppositely charged ions is $E=-(Q_AQ_B)/(4\pi\varepsilon r)$, where Q_A and Q_B denote the charges and r is the interatomic distance.

Exopolymer
A biopolymer secreted by a microbe into its environment.

Fluid–fluid phase separation
This resembles the physical separation of two fluids like vinegar and oil; in coacervation, molecules are initially completely soluble in water but, upon neutralizing one another, coalesce over time to form a separate oil-like fluid.

Lewis base
In the Lewis theory of acids and bases, a Lewis base is a compound that donates a pair of electrons. In the formation of Δ-Dopa from Dopa-quinone, a Lewis base enables extraction of a proton from -CH_2- in the side chain, thereby freeing up a pair of electrons to restore the aromatic ring. Phosphate, carbonate, glutamate anions are all Lewis bases.

Macroion
Usually a polyelectrolyte or large molecule such as a protein bearing many charges.

Microion
A small ion such as Na^+ or Cl^- serving as countercharge to charges on a macroion.

Solubility product (K_{sp})
A constant used to describe ionic compounds of relatively low solubility. An example, Fe(III) phosphate, dissociates poorly in water as $FePO_4$ (s) ⇆ Fe^{3+} (aq) + PO_4^{3-} (aq); in saturated solutions at equilibrium, the $K_{sp}=[Fe^{3+}]^1[PO_4^{3-}]^1=1.3\times10^{-22}$ at 25°C.

depression of the foot. Thread formation occurs in the ventral groove and resembles injection molding of collagenous liquid crystals (Waite, 1992; Hassenkam et al., 2004), whereas injection molding of the plaque in the distal depression produces a porous solid. During thread formation, byssal proteins are secreted incrementally along a distal to proximal trajectory. Plaque proteins, beginning with those at the distal end between the foot-tip and substratum, are deposited first, followed by the bulk of the plaque and thread core components (Yu et al., 2011b; Petrone et al., 2015). Finally, just before the thread disengages from the groove, the assembled structure is coated by a ∼5-µm-thick cuticle from the accessory gland, whereupon the new thread is recruited into load-bearing service (Fig. 1C).

Adhesive protein diversity and modification

Although not yet fully characterized, the byssus has as many as 20 different known protein components, most with highly localized distributions. Byssal proteins, particularly mussel foot proteins (Mfp)-2, -3, -4 and -5, originate from the phenol gland and are destined for the plaque (Fig. 1D). Evidence for phenol gland localization of Mfp-2 and Mfp-3 is based on *in situ* hybridization (Miki et al., 1996; Inoue et al., 1996), and suggests that different parts of the phenol gland express different proteins. Mfp-1 has been localized to the accessory gland (Miki et al., 1996) where, according to transcriptomic analysis, Mfp-6 also resides. Collagen gland proteins, such as the prepolymerized collagens (preCOLs), with distal (D), proximal (P) and nongradient (NG) distributions (preCOL-D, -P and -NG) and thread matrix proteins TMP and proximal TMP (PTMP) are destined for different parts of the thread core (Sagert and Waite, 2009). Transcriptomic analyses of the mussel foot suggest that additional byssal precursor proteins exist, but these are not yet fully isolated and characterized (D. DeMartini and J.H.W., unpublished results), although the cationic, aromatic and glycine-rich hallmarks of the known Mfps are in evidence. Table 1 summarizes all known *Mytilus* byssal proteins, their origin in the foot and their localization in the byssus. Although Mfps do exhibit some chemical diversity, most are glycine rich and contain Dopa, and all are moderately to strongly cationic (Fig. 1E,F). A complete compilation of known byssal protein sequences has been reported elsewhere (Lee et al., 2011). Given the probable repulsion between cationic Mfps, particular efforts have been made to find and isolate potentially neutralizing polyanionic proteins from byssus; however, these have not succeeded. In the marine cement of *Phragmatopoma californica* (Zhao et al., 2005), which has much in common with mussel adhesive proteins, such polyanionic proteins are created by phosphorylation of uncharged serine-rich precursors. In mussels, Mfp-5 undergoes similar phosphorylation but serine levels are typically lower (Fig. 1E, pSer) than in *Phragmatopoma* (Lee et al., 2011).

Besides pSer formation, post-translational modification of the Mfps and preCOLs is varied and extensive, affecting up to 60% of all amino acids in Mfp-1, indicating enzyme-dependent co- or post-translational processing. Some modifications are associated with well-studied enzymes (e.g. production of *trans*-4-hydroxyproline by prolyl-4-hydroxylases), but the enzymes that modify Mfps are likely to be genetically distinct from the collagen-specific prolylhydroxylases (Guzman et al., 1990). This may also apply to the kinases that phosphorylate serines in Mfp-5 and Mfp-6 (Qin and Waite, 2001; Zhao and Waite, 2006). Other modified amino acids, such as Dopa and 4-hydroxyarginine, suggest the existence of new enzymes such as 3-tyrosyl- and 4-arginyl-hydroxylases, although these have yet to be characterized. Recent transcriptomic analysis of the byssome in *Perna viridis* (a mytilid), has uncovered two tyrosinase-like sequences (Guerette et al., 2013), but their distinct hydroxylase and oxidase activities are undetermined.

Most *Mytilus* plaque proteins start out as intrinsically disordered to some degree (Table 1). Mfp-3, Mfp-5 and Mfp-4 have little

Journal of Experimental Biology (2017) 220, 517-530 doi:10.1242/jeb.134056

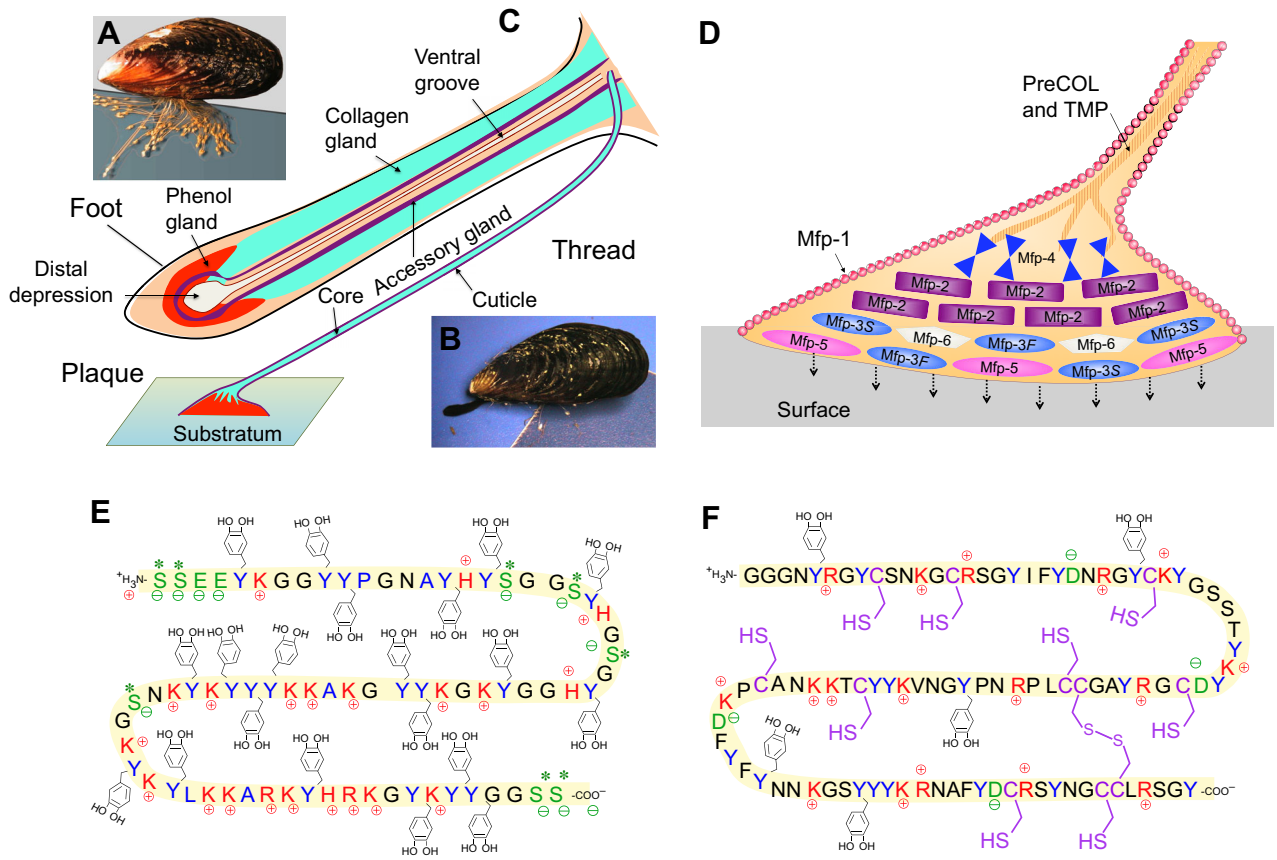

Fig. 1. Attachment process of *Mytilus* mussels to a surface. (A) The mussel byssus contains hundreds of threads proximally fused to muscle at the base of the foot and distally attached to the substratum. (B) To make a new thread, the foot emerges from the living space within the mussel shell and touches a surface. (C) Reminiscent of reaction injection molding, molecular precursor proteins of byssus are conducted to and assemble within the ventral groove and distal depression of the foot. Three gland clusters – phenol, collagen and accessory glands – synthesize and stockpile specific byssal proteins. (D) Schematic representation of the distribution of known proteins in the byssal plaque and distal thread. (E) Sequence of Mfp-5 from *Mytilus edulis*, showing the prominence of Dopa (Y-methyl catechol), Lys (K), Ser (S) and Gly (G). (F) Sequence of Mfp-6 from *M. californianus* with abundant Cys (C), Arg (R) and Lys (K), Gly (G) and Tyr (Y). Color key: Tyr/Dopa (blue), cationic side chains (red), anionic side chains including phosphoSer (green) and thiols (purple). Sequences from Lee et al., 2011.

detectable solution structure at pH 3. Both Mfp-1 and Mfp-2 have local structure – such as polyproline II and an epidermal growth factor-like motif, respectively – connected by disordered sequences (Olivieri et al., 1997; Hwang and Waite, 2012; Mirshafian et al., 2016). preCOLs are trimeric with super-secondary triple helical collagen cores flanked by silk-like β-sheets in preCOL-D, and disordered elastin in preCOL-P and preCOL-NG (Arnold et al., 2012). It is highly probable that a different structure is gained upon pH-induced precipitation, as for variants of Mfp-3 (Wei et al., 2013a; Mirshafian et al., 2016; Petrone et al., 2015), which gain β-sheet structure during titration from pH 3 to 7.5.

Table 1. Comparison of the known proteins of *Mytilus byssus* with regard to localization in the foot glands and byssus, mass, structure, modification and adhesion to mica

Protein	Localization (gland→ byssus)	Mass (kDa)	Structure	Modifications (mol%)	E_{ad} (mJ m^{-2})
Mfp1	Accessory→ cuticle	~110	Disordered; PPII	Dopa (15) Hyp; DiHyp	1
Mfp-2	Phenol→ plaque core	45	Disordered; EGF	Dopa (5)	1
Mfp-3F	Phenol→ plaque interface	6	Disordered	Dopa (20) HOArg	6
Mfp-3S	Phenol→ plaque interface	6	Disordered	Dopa (10)	3
Mfp-4	Phenol→ plaque core	90	Disordered	Dopa (2)	0
Mfp-5	Phenol→ plaque interface	11	Disordered	Dopa (30); pSer	15
Mfp-6	Phenol→ plaque interface	12	Disordered; beta	Dopa (5)	0.5
Mfp-7	Phenol→ plaque core	35	n.d.	Dopa (0.2)	n.d.
preCOL-D	Collagen→ thread core (distal)	240 (trimer)	Collagen core; silk	Hyp; Dopa (0.1)	n.d.
preCOL-P	Collagen→ thread core (proximal)	240 (trimer)	Collagen core; elastin	Hyp; Dopa (0.1)	n.d.
preCOL-NG	Collagen→ thread core	240 (trimer)	Collagen core; Glycine rich	Hyp; Dopa (0.1)	n.d.
PTMP-1	Collagen→ thread core (proximal)	45	vWF fold	Glycosylation	n.d.
TMP-1	Collagen→ thread core	56.5	Disordered	Dopa	n.d.

PPII, polyproline II helix; EGF, epidermal growth factor; vWF, von Willebrand factor; HOArg, hydroxyarginine; Hyp, hydroxyproline; diHyp, dihydroxyproline; pSer, phosphoserine; trimer, mass corresponds to the trimer; adhesion energy E_{ad} is a mean of 3–5 samples; s.d. is ±10% of mean. n.d., not determined.

Journal of Experimental Biology (2017) 220, 517-530 doi:10.1242/jeb.134056

Deposition process

Foot-tip cavitation

Byssal protein is deposited from the foot during surface contact (Fig. 2A). The distal portion of the foot is first pressed against a surface to secure a perimeter of contact, then, by raising the ceiling, a negative pressure is created (Fig. 2B). Suction provides temporary attachment to the surface, but may also serve to draw adhesive proteins from the conducting tubules through six or more pores in the ceiling of the distal depression onto the target surface (Tamarin et al., 1972). Cavitation of foot tissues in cephalopod and gastropod molluscs generates hydrostatic pressures below 0 kPa (Kier and Smith, 2002; Smith, 1991), but these have yet to be quantified in mussels (note that atmospheric pressure at sea level is 101 kPa). Foot attachment is capable of supporting the weight of a mature 150 g mussel (*M. californianus*) in air (Hwang et al., 2010b). Mussels avoid attaching to substrates containing pores with diameters less than the diameter of the distal depression (~2 mm in a mature mussel; W. Wei, Q. Zhao and J.H.W., unpublished results). Presumably this is because negative pressures leak on pore-containing surfaces.

pH and ionic strength

Given that mussels are thoroughly adapted to seawater habitats, attachment chemistry was widely assumed to occur under seawater conditions, i.e. pH 8 and ionic strength of 0.7 mol l^{-1}. In fact, mussels impose distinct conditions during substrate preparation just prior to secretion of their adhesive proteins (Fig. 2C). Deposition pH and ionic strength (conductivity) have been monitored using microelectrodes and reporter dyes, with different results. With a microelectrode inserted into the distal depression of the foot during plaque protein secretion, pH averaged 5.5 (pH range 4–6.5) (Yu et al., 2011b) and ionic strength was 0.15 mol l^{-1}, which is typical for cells and body fluids. In a later study, a pH-sensitive surface was prepared by tethering a pH-dependent fluorescent dye to a surface presented to juvenile mussels for attachment (Martinez-Rodriguez et al., 2015); fluorescence and pH were then measured using

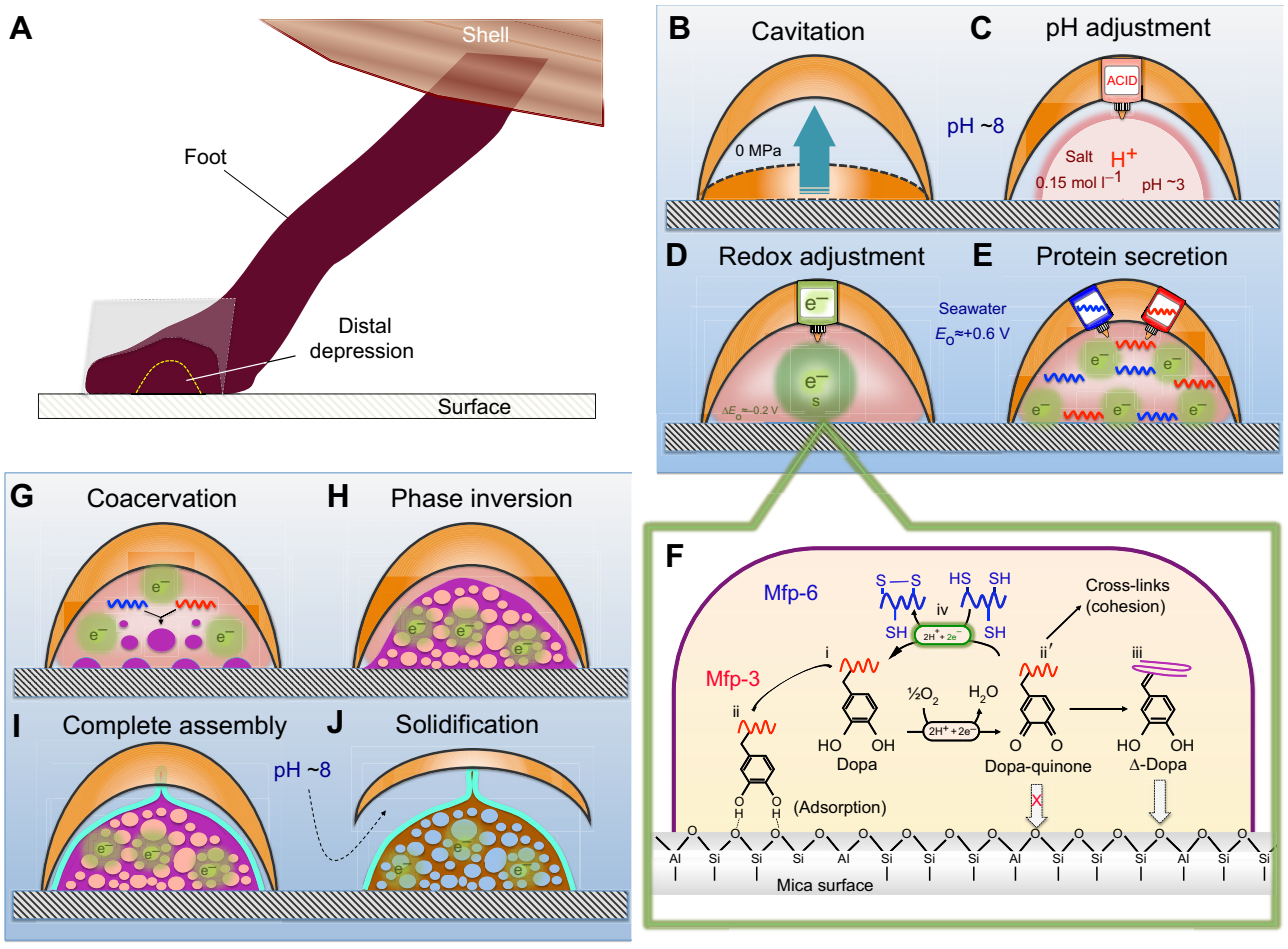

Fig. 2. Plaque protein deposition by the foot. (A) The inverted cup shape represents a 2D cross-sectional view of the distal depression in contact with a target surface for adhesion. Labeled panels show the stages of plaque protein deposition. (B) Cavitation or creation of negative pressure between foot and surface. (C) Secretion of acid to pH as low as ~2. (D) Redox regulation. (E) Release of adhesive proteins (red and blue) and adsorption to target surface. Because Dopa-rich proteins help to adjust redox, the difference in timing of D and E may not be significant. (F) Redox activity driven by the difference between the high pH and O_2 concentration of seawater versus the low pH and abundance of electron donors in the plaque: (i) Adhesive protein Mfp-3 (red) or Mfp-5 is deposited and (ii) binds to the target surface; as Fe^{3+} or O_2 leaks in, some Dopa is oxidized to (ii′) Dopa-quinone, which is poor in adhesion but active in cross-linking (cohesion). (iii) At increasing pH, Dopa-quinone can self-reduce to Δ-Dopa (with conformational effects). (iv) Dopa can also be rescued by reduction using electrons from thiolates in Mfp-6. Not shown is the favorable scavenging reduction of O_2 by Mfp-6 (blue) thiolates. (G) Coacervation: proteins undergo fluid–fluid phase separation. (H) Coacervate/water phase inversion. (I) Plaque assembly is completed and a protective cuticle is added over the plaque. (J) Solidification of fluid.

Journal of Experimental Biology

confocal microscopy. The pH minimum averaged ∼2.5 and ranged from 2 to 4.

The differences in the two methods probably reflect factors such as timing and location. The measured reporter dye pH was strictly interfacial and detected pH changes 2–5 s after foot placement, whereas the electrode pH provides an average measurement for a volume of ∼20 µl at 1 min post-secretion. Byssus acidification is assumed to involve proton pumping, such as that reported for stomach acidification by H^+/K^+-ATPase (Shin et al., 2009), but the actual mechanism is unknown. There are reports of acidic secretions coupled with sulfate anions from molluscan foot tissues (Thompson, 1983). None, however, have been investigated in any chemical detail. The actual functions of acidity remain obscure – all of the following are relevant hypotheses about byssal acidification, and they are not mutually exclusive: (1) acidity etches/cleans the surface; (2) acidity kills surface-absorbed microbes; (3) acidity titrates surface-active groups for adhesion; (4) acidity regulates the redox environment of the plaque, and (5) acidity is used to control protein fluidity, phase inversion and precipitation. Many of these hypotheses are discussed below. In particular, the role of acidity as a precondition for initial adhesion is discussed below in 'Surface physics'.

Redox

O_2-saturated seawater is highly oxidizing at between +0.6 and +0.8 V (standard hydrogen electrode) (Cooper, 1937). The strongly positive redox potential is correlated with the half-reaction: $½O_2+2e^-+2H^+ \rightarrow H_2O$, and predicts that the affinity of oxygen for electrons will eventually succeed in oxidizing most forms of organic carbon. Living cells avoid this by creating reducing reservoirs and by tapping into the favorable free energy released by O_2 reduction to make ATP. Mfps that contain thiols (Cys) and catechols (Dopa) are shielded against oxidation during their cellular storage, but they become susceptible upon secretion. Although oxidation of Dopa to Dopa-quinone was once thought to be essential for protein cross-linking and cohesion in byssus, unoxidized Dopa is now known to be equally important for adhesion. To maintain both reduced and oxidized forms, stringent, location-specific redox control is necessary. Mussels impose strong reducing conditions under the foot during the deposition of new plaques (Fig. 2D). Assuming that O_2 is excluded during deposition, and that catechols and thiols are a thousand times more abundant than their corresponding oxidized forms (quinones and disulfides, respectively), the initial secretion is estimated to be at least 200 mV more reducing than seawater (Fig. 2F). How long this difference persists, particularly after foot lift-off, whereupon the plaque equilibrates with ambient seawater O_2, is a matter of considerable interest. Indeed, a recent study showed that a silica surface saturated with a redox sensor was reductively bleached by contact with freshly exposed 21-day-old plaque undersides, i.e. the plaque portion facing the substratum (Miller et al., 2015).

Mfp-6 is largely responsible for the reducing activity of the plaque, with a capacity of at least 17 electrons per molecule of Mfp-6 at pH 3 (Nicklisch and Waite, 2012; Nicklisch et al., 2016). Nine cysteine thiols and four Dopa residues contribute to the reservoir of reducing electrons, but little is known about the sequence of reactions involved, particularly the flow of electrons (Mirshafian et al., 2016). Many Mfp-6 thiol and Dopa residues have reducing redox potentials of about −0.22 and +0.25 V, respectively, that are capable of sacrificially reducing either O_2 or Dopa-quinones. The overall effect of maintaining a reducing environment is summarized in Fig. 2F. (1) Dopa-rich adhesive proteins are secreted by the foot; (2) some proportion of the Dopa adsorbs to form bidentate complexes with the surface; (3) owing to trace O_2 or Fe^{3+} present, unadsorbed Dopa undergoes a one- or two-electron oxidation to Dopa-quinone (Barrett et al., 2012), which has poor surface bonding properties; to decrease Dopa-quinone's tendency to undergo oxidation, mussels have evolved two rescue pathways: (4) Dopa-quinones tautomerize to dehydroDopa, or (5) thiolates in Mfp-6 donate electrons to restore Dopa from quinone.

The peculiar tautomerization of Mfp-Dopa-quinone is essentially a 'self-reducing' behavior (Fig. 2Fii′–iii). At pH 6–8, in the presence of a Lewis base (see Glossary), electrons in the side-chain are recruited into the ring for quinone reduction back to catechol (Mirshafian et al., 2016). The new catechol, however, is no longer Dopa but a vinyl catechol known as α, β-dehydro (Δ)-Dopa (Rzepecki et al., 1991). Because the catecholic moiety has been restored, many (but not all) properties of parent Dopa [e.g. metal complexation, reoxidation, hydrogen (H)-bonding] are again available. However, Δ-Dopa has an oxidation potential that is 100 mV more cathodic (easier to oxidize) than that of Dopa, and the formation of a vinylic double bond has consequences for protein conformation (Mirshafian et al., 2016). Probably, the oxidation of Δ-Dopa serves to add electrons to the reducing reservoir of Mfp-6 in a 'last ditch' effort to extend the lifetime of interfacial catechols and adhesion after which the plaque becomes obsolete (Mirshafian et al., 2016). Important questions about plaque redox are whether it ever equilibrates with seawater, and, if not, how a distinct redox environment is maintained in the plaque. Because much of adhesion chemistry occurs under non-equilibrium conditions, redox in plaques is likely to be kinetically, not thermodynamically, controlled.

Protein secretion and fluid–fluid phase changes

Each new byssal thread starts as a protein-rich fluid that is reaction-injection-molded by the foot along a distal to proximal trajectory. The initial sequence of protein deposition at the distal end around the plaque has been investigated by time-lapse mass spectrometry (Yu et al., 2011; Petrone et al., 2015). Following acidification of the distal depression, Mfp-3 variants, Mfp-5 and Mfp-6 are secreted within seconds of one another. These proteins undoubtedly adsorb to surfaces as solutes, but they also undergo condensation as fluid–fluid phase separations (see Glossary) (Wei et al., 2013a) (Fig. 2G). Condensation can lead to ordered or intrinsically disordered fluids (liquid crystals or coacervates, respectively) and is entropically favored by the release of water and microions (see Glossary).

Complex coacervation is a common fluid–fluid phase separation that occurs upon mixing two polyelectrolytes at a pH where they electrically neutralize one another (Bungenberg de Jong, 1949). For example, mixing a lysine-rich protein, such as histone, with a negatively charged phosphoprotein (Aumiller and Keating, 2016) at a pH and concentration where the positive charges on one exactly counteract the negative charges on the other, leads to their fluid–fluid phase separation from equilibrium solution, initially as microdroplets that coalesce with one another, eventually forming a dense bulk phase (Fig. 2G).

Coacervates are metastable, but have excellent transient physical properties for underwater adhesion: (1) they are denser than water and so can be directly applied to a surface without being diluted by diffusion; (2) they have low (<1 mJ m^{-2}) interfacial energies, enabling them to spread over wet surfaces; (3) they have high internal diffusion coefficients, resulting in good mixing for cargo such as enzymes (e.g. catecholoxidase); and (4) they possess shear-thinning viscosities that are an order of magnitude lower than viscosities associated with uncondensed molecules at the same

concentration, which would improve flow through narrow conduits (e.g. conducting tubules during delivery) (Hwang et al., 2010b).

Fabrication of a solid load-bearing material from water-soluble precursors in ∼5 min, outside the confines of living tissue depends on macromolecules with unusual and controllable phase behavior. Protein coacervation is increasingly implicated in the phase behavior and processing of Mfps in plaques. Optimizing pH, ionic strength and polyelectrolyte concentrations for coacervation *in vitro* typically requires the construction of phase diagrams (Chollakup et al., 2013), and phase diagrams of synthetic polyelectrolytes have been prepared to mimic complex coacervation in sandcastle worm (*Phragmatopoma californica*) cement, where two families of phosphoserine- and lysine-rich proteins come together as coacervated underwater adhesives, and eventually precipitate, which represents another important phase change (Shao and Stewart, 2010).

Coacervation of mussel adhesive proteins involves single components rather than paired oppositely charged molecules, and is not necessarily charge neutral. The best-studied single-component coacervate in *Mytilus* is Mfp-3S, an abundant Mfp-3 variant (Wei et al., 2013a,b). Coupling of oppositely charged sites in Mfp-3S sets up additional H-bonding and hydrophobic interactions that result in fluid–fluid phase separation, but the ensuing phase behavior needs more scrutiny. Apparently, the charge neutrality of macroions (see Glossary) is not necessary for coacervation of certain types of polyelectrolytes; indeed, Kim and co-workers (2016) recently reported that coacervation of mussel-adhesive inspired aromatic polycations can overcome long-range repulsions by extensive cation-π interactions (see Glossary), which are further discussed below.

Coacervates are fluids, unlike byssal plaques, which are solid porous materials (Fig. 2G–J). It is conceivable that coacervates solidify by protein cross-linking, but the formation of a porous microarchitecture is more of a stretch. Many synthetic polymers are capable of another kind of phase change: phase inversion (Fig. 2H). Rather than being a dispersion of coacervate microdroplets in water (i.e. water is the continuous phase, coacervate is discontinuous), in phase inversion, water droplets become dispersed within the continuous coacervate. Phase inversions are common in the manufacture of polymeric membranes and typically are driven by changes in interfacial energy, viscosity and surface area between the phases (Strathmann and Kock, 1977). A recent investigation of a synthetic coacervate model system inspired by mussel adhesion revealed that complex coacervates can undergo phase inversion to form a structured fluid; the continuous inverted fluid phase then hardens to form a load-bearing porous material (Zhao et al., 2016). The relevance of these results to plaque formation remains to be demonstrated with plaque proteins. Of particular interest is timing: do phase inversion (Fig. 2H) and solidification (Fig. 2J) happen before or during foot lift-off? (Fig. 2I,J).

Surface physics

Adhesion is about joining different materials, whereas cohesion is the joining of similar materials. Practical adhesives, including byssus, must carefully balance adhesion and cohesion for best performance. During mussel adhesion, release of a mixture of proteins – as solutes and/or coacervates – into the distal depression is the first step towards bonding to a target surface. The imposed conditions (acidic pH, low ionic strength, reducing redox) are different from those of seawater. The adhesion of Mfp proteins, peptides and even single amino acid residues to well-defined surfaces has been investigated and quantified using atomic force microscopy (AFM) and the surface forces apparatus (SFA; Table 1). Protein nanometer-scale adhesion differs from practical adhesive bonding in being dominated by surface physics where each molecule has domains or functionalities attached to both surfaces. Typical configurations for testing protein adhesion are described as symmetric or asymmetric (Fig. 3A). Adhesion is usually tested in an asymmetric configuration, involving adsorption or tethering of a biomolecule or a film one molecule thick to one mica surface, then measuring the force as a function of intersurface distance relative to an apposing uncoated surface upon approach (‘in’), followed by separation (‘out’) (Fig. 3B). By convention, a force is considered repulsive when positive and attractive when negative; during approach, the minimum distance between compressed surfaces approximates the diameter of hydration in the protein monolayer (Danner et al., 2012) (Fig. 3B). When the repulsive force increases with no change in the distance, approach is reversed and separation begun. A negative force during separation indicates adhesion; adhesion force (F) is typically converted to adhesion energy (E_{ad})

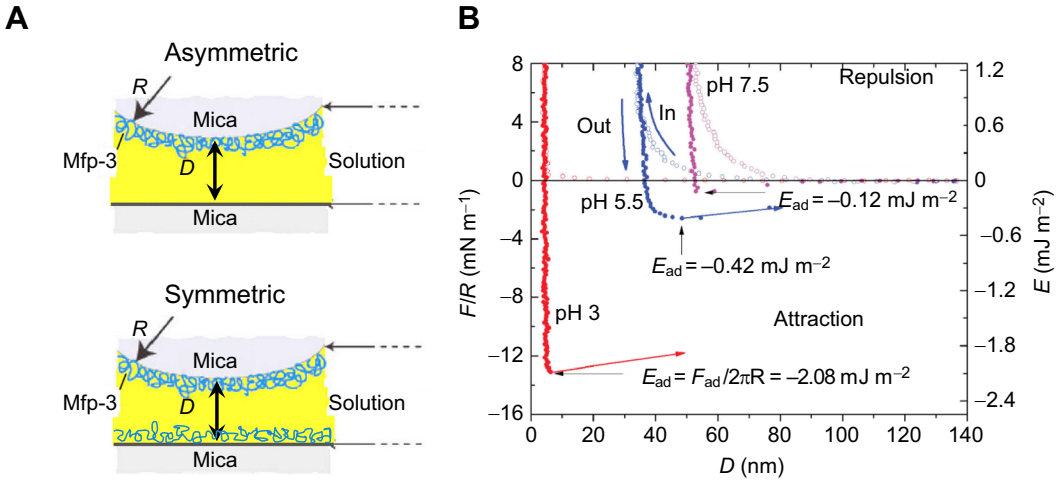

Fig. 3. Measuring and comparing the molecular adhesion of plaque proteins on mica (muscovite) surfaces. (A) Two configurations for testing the adhesion and cohesion of proteins in the surface forces apparatus (SFA). Asymmetric means that a protein monolayer (blue) is applied to one surface only, whereas in the symmetric configuration protein is applied to both surfaces. *D*, distance; *R*, radius. (B) Adhesive (asymmetric) performance of Mfp-3F in the SFA at different pH values. ‘In’ denotes the approach of two surfaces, whereas ‘Out’ denotes separation. Adapted from Yu et al., 2011a,b.

Journal of Experimental Biology (2017) 220, 517-530 doi:10.1242/jeb.134056

using the Derjaguin equation $E_{ad}=F_{ad}/2\pi R$, where R is the radius of curvature in the glass cylinders to which the mica surfaces are mounted (Israelachvili, 2011). The symmetric configuration involves protein adsorption to both mica surfaces and is sometimes useful for investigating cohesive interactions; if protein adhesion to mica is very strong, the cohesive interactions between the two films will usually yield before separation at the interface (Fig. 3A).

Mica is the most popular experimental substratum in adhesives research because it is atomically smooth and its surface chemistry is highly reproducible when freshly cleaved, which is particularly important for identifying chemical contributions to adhesion. As an aluminosilicate mineral (muscovite), mica is also ecologically relevant to the intertidal zone where mussels live. Mica can also be converted to a variety of other surface chemistries using electron-beam deposition and self-assembled monolayers (Yu et al., 2013a,b; Lu et al., 2013b).

The adhesion of various Mfps to mica has been measured using SFA (Lee et al., 2011; Table 1); here, cohesion is provided by the covalent protein backbone so that failure is shifted to the interface. Strongest adhesion is associated with monolayers of the purified proteins Mfp-3F and Mfp-5, and both force and energy of adhesion to mica are closely correlated with pH (Fig. 3B; Table 1). The greatest Mfp-5 adhesion energies, at pH 2–3, exceed those of streptavidin–biotin (-10 mJ m^{-2}), which act as a benchmark of noncovalent interactions in proteins (Helm et al., 1991). Adhesion peaks at pH 3 but shows a log decay with increasing pH. Remarkably, after raising the pH to 7.5, Mfp-3 adhesion is only 5% of that exhibited on mica at pH 3 (see below).

Adhesive chemistry at acidic pH

Most surfaces are highly changeable in seawater. On a metal surface, for example, the following occur in quick succession: (1) oxygen is chemisorbed (see Glossary), often producing metal oxide or hydroxide; (2) water is adsorbed (hydration layer ~0.5 nm thick), along with hydrated salts; (3) a conditioning film consisting of low molecular weight adsorbates such as phenolics, fatty acids and simple saccharides develops; (4) microbes come to feed on this film; and (5) microbial communities make complex biofilms or exopolymers (see Glossary) (Loeb and Neihof, 1975; Schneider, 1996; Callow and Callow, 2006). The exopolymers on actual surfaces are short-lived because they are consumed by grazers (e.g. gastropods) or sloughed off in microspatial patches to re-expose the underlying chemistry (Hutchinson et al., 2006). Although adhesion to naturally fouled surfaces must eventually be investigated, all real surfaces are currently assumed to be patchy, and interfacial chemistry is best obtained from well-defined solid surfaces.

A long-standing aim of research on mussel adhesion is a fundamental understanding of interfacial chemistry. At pH 2–3, even before interfacial bonding takes place, there are measurable changes in surface hydration. For example, dynamic investigations of synthetic Mfp-3 adsorption to titanium dioxide (titania) and hydroxyapatite (HAP) surfaces show that Dopa-containing Mfp-3 peptides evict surface hydration layers from both surfaces, whereas those with tyrosine do not (Wei et al., 2016). A similar effect of catechol on hydrated silica is also predicted (Mian et al., 2014). Surface dehydration is even more extensive using coacervated Dopa-peptides, suggesting a synergy between Dopa and the coacervated fluid state. Surface hydration is also reduced by lysine- and catechol-rich siderophore homologs of Mfp-5 (Maier et al., 2015). Charged lysine plays a subtle but indispensable role in evicting hydrated surface cations from aluminosilicates (Maier et al., 2015). On mica, for example, hydrated K^+ sits over alumina sites, thereby blocking them from being coordinated by the catecholate moiety of Dopa (McBride and Wesselink, 1988). By removing these cations, lysine enables Dopa surface binding.

At acidic pH, particularly below the pK_a of most organic acids, the H-bond is predictably the most abundant interaction on polar surfaces including mica, silica, titania and HAP (Wei et al., 2016) (Fig. 4A). Although comparatively weak, the bidentate H-bond of Dopa is notable for its bond lifetime, which is ~10^6 times longer than that of the monodentate (Yu et al., 2011a), thus ensuring that once Dopa is ‘on’, the probability of protein desorption is low. Dopa-peptides are extensively H-bonded to titania and HAP surfaces at acidic pH (Wei et al., 2014, 2016). To better define how much Dopa contributes to H-bonding, researchers have attempted to ‘knockout’ Dopa of Mfp-3 and Mfp-5, by oxidation to Dopa-quinone (which can no longer H-bond to the surface) at acid pH. Losses in Mfp adhesion to mica were commensurate with

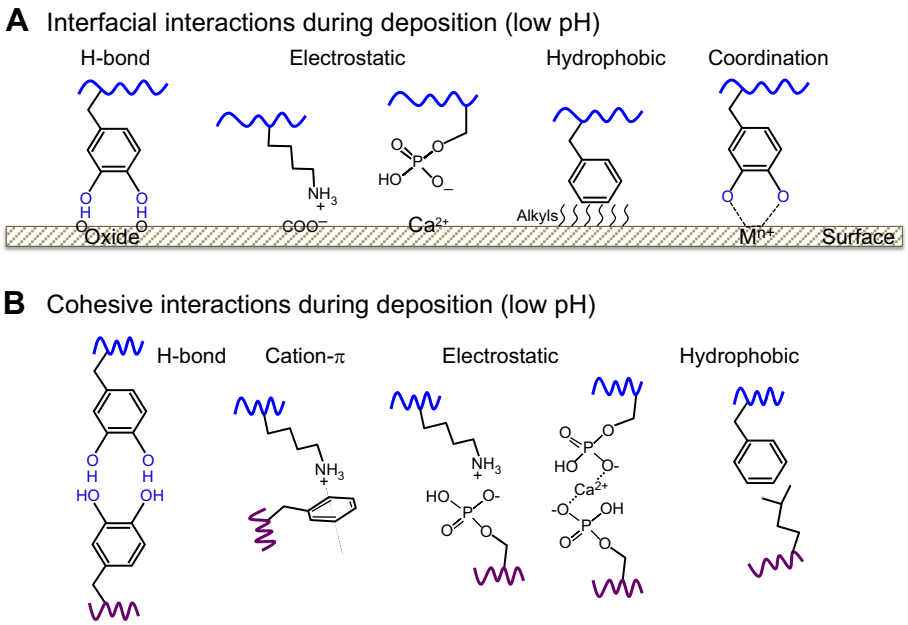

Fig. 4. Plaque adhesive chemistry under the foot at acidic pH. (A) Interfacial interactions: H-bonds, and electrostatic, hydrophobic and coordinative interactions. The latter are uncommon at pH 2–3. (B) Cohesive interactions: H-bonds, cation-π interactions, electrostatic (e.g. salt bridges) and hydrophobic interactions.

Journal of Experimental Biology (2017) 220, 517-530 doi:10.1242/jeb.134056

the extent of conversion (Yu et al., 2011a,b; Danner et al., 2012). The most biologically relevant evidence to support a leading role for Dopa-mediated adhesion is 'reductive' rescue: adhesive losses attributed to Dopa oxidation are completely reversed by adding reducing agents, particularly Mfp-6, which has poor adhesive tendencies by itself (Yu et al., 2011a). In summary (Fig. 4A), interfacial interactions of the plaque with the substrate implicated at acidic pH include: bidentate H-bonding (Yu et al., 2011a), electrostatic attraction (Wei et al., 2013a,b) and hydrophobic interactions (Yu et al., 2014); coordination (see Glossary) is limited to pH≥5.

Using the symmetric configuration in the SFA, several interactions have emerged as significant in cohesion between Mfps (Fig. 4B): (1) bidentate intercatechol H-bonding is robust in aqueous solution (Ahn et al., 2014); (2) cation-π interactions between Lys and Dopa, Phe, Tyr or Trp, which are surprisingly cohesive in the Mfps (Lu et al., 2013a); (3) Ca^{2+} salt bridges between paired pSer residues (i.e. electrostatic interactions), which were first noted in *P. californica* cement but are reckoned to be more widespread (Zhao et al., 2005; Ashton et al., 2011); and (4) hydrophobic interactions (Yu et al., 2013a).

The byssal plaque: maturation post-foot lift-off

The plaque proteins contribute little to holdfast tenacity while the foot is down and pH is acidic. However, once the foot disengages, the nascent structure gains shape, solidity, microarchitecture and durability. Here, I discuss recent work on the structure and properties of mussel byssal plaques following their disengagement from and release by the foot, and their equilibration with the surrounding seawater. I begin by discussing the architecture of mature plaques, then go on to consider the tensile properties of plaques, interfacial and cohesive chemistry in seawater and the interplay of chemistry and mechanics.

Architecture of mature plaques

Exposure to seawater during foot disengagement is the switch that causes new byssal threads and plaques to solidify. The structural components of solidified byssus range in scale from micrometers to centimeters, and contribute to adhesion in ways that are often independent of chemistry (Fig. 5).

At the centimeter scale, the radially distributed stiff-to-compliant threads in each mussel byssus (Fig. 5A) increase 900-fold in tenacity under dynamic loading relative to static loading (Bell and Gosline, 1996; Qin and Buehler, 2013). At the millimeter scale, the spatulate morphology of each adult thread (which expands from a diameter of <0.1 mm to >2 mm at the plaque) (Fig. 5B) increases adhesion, as spatulate morphologies exhibit 20-fold stronger adhesion than untapered cylinders with the same interfacial surface contact area (Spuskanyuk et al., 2008). Mature plaques also have extensive microstructure that is probably acquired by

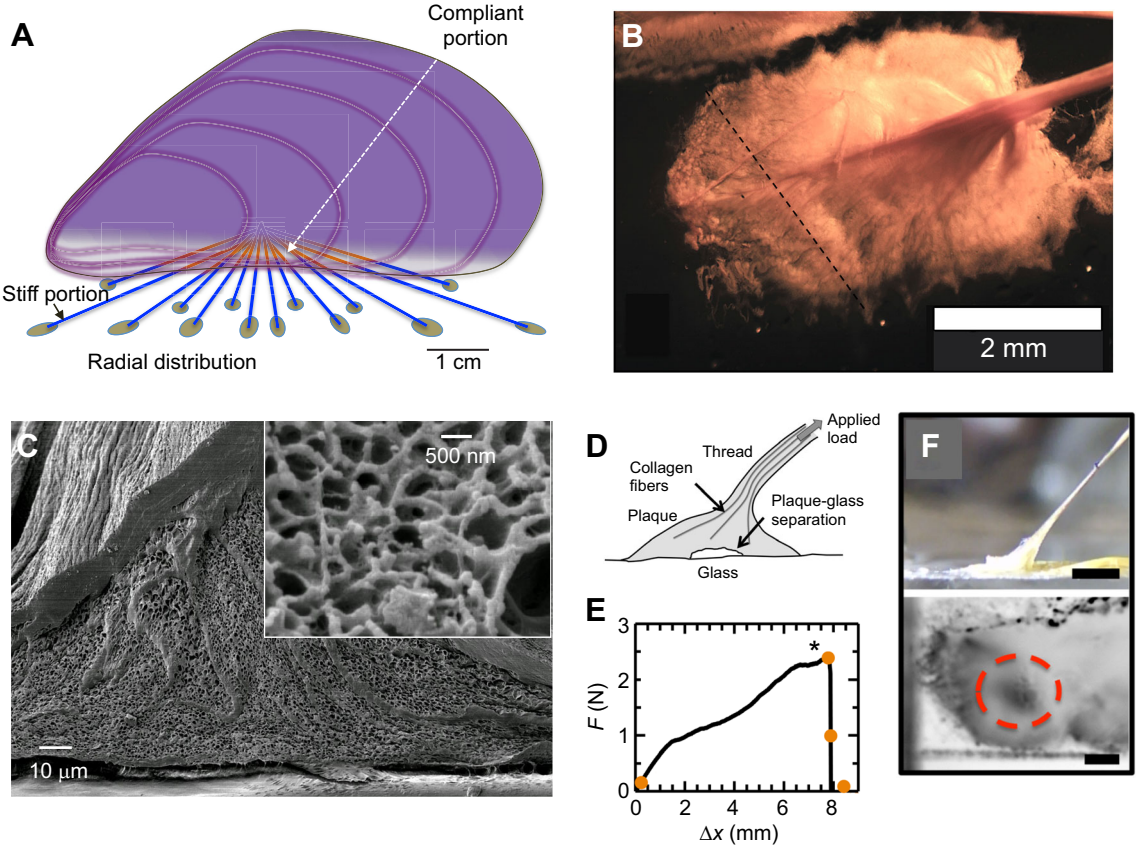

Fig. 5. Higher length scales of structure also improve adhesion performance. (A) Radial distribution of threads having a distal to proximal stiffness gradient. The stiff portion is in blue and the compliant portion is in orange. The compliant portion is typically concealed within the valves. (B) The spatulate geometry of a byssal thread and plaque [dashed line shows orientation of section for scanning electron microscopy (SEM) shown in C]. (C) The trabecular (spongy) structure of a plaque in SEM section. (D–F) The fracture mechanics of individual whole plaques in tension. (D) Schematic diagram of a plaque cross-section during tension. (E) Tensile force–deformation plot of a single plaque. (F) Photographic side (top) and underside (bottom) views of deformation in a plaque at point marked by asterisk in E are shown. Scale bars: 1 mm. Red circle indicates locus of plaque separation from the surface as sketched in D. The fracture energy G_c is derived from the force F_c by $F_c/b=G_c/(1-\cos\theta)$, where b and θ denote width and pull angle, respectively. Adapted from Desmond et al., 2015.

Journal of Experimental Biology (2017) 220, 517-530 doi:10.1242/jeb.134056

phase inversion and protein precipitation during foot lift-off (Tamarin et al., 1972; Filippidi et al., 2015). A mature plaque is a skin-covered fiber-reinforced porous solid, with pore dimensions of two length scales (100 nm and 1000 nm) (Filippidi et al., 2015) (Fig. 5C, inset). Plaque fibers are splayed continuations of preCOL bundles in the thread, and the skin consists at least partly of Mfp-1 complexed with Fe^{3+} (Harrington et al., 2010). The contribution of plaque microstructure to adhesive performance has yet to be determined, but a large body of evidence shows that porous or 'cellular' solids often toughen structural adhesives by stopping cracks, enabling reversible deformation and increasing energy dissipation (Ashby, 1983). They are also more economical because less polymer is needed to fill a given volume.

Tensile mechanics of mature plaques

Although adhesive tensile testing of mature byssal plaques has been undertaken previously (Allen et al., 1976; Burkett et al., 2009; Crisp et al., 1985), a recent study by Desmond et al. (2015) was the first to combine mechanics with video recordings of plaque deformation to the break point under tension at different angles and strain rates. The results revealed an unexpectedly large discrepancy between plaque and molecular adhesion. For example, comparing the best interfacial adhesion energy by Mfp-5 ($\leq$20 mJ m^{-2}; Table 1) with the best actual fracture energy of single-notched plaques attached to glass (Fig. 5D; ~200 J m^{-2}) reveals a 10,000-fold difference. Of course, the two tests are not measuring quite the same energy, but it is important that these energies are different.

Using a specially engineered tensiometer, Desmond et al. (2015) studied two types of failure modes in *Mytilus* plaques: adhesive and cohesive modes, which are both associated with extensive deformation before failure. The adhesive mode starts with the separation of the plaque–substratum interface near the center of the plaque with a peel-like separation expanding radially (Fig. 5D). The cohesive failure, in contrast, starts at an internal singularity, such as a large pore or flaw that expands until catastrophic breakage occurs. Several studies that have cycled stress–strain suggest that byssal deformations are reversible up to a certain strain (Holten-Andersen et al., 2007; Carrington and Gosline, 2004).

Plaque chemistry: different in seawater

As discussed above, important chemical interactions during plaque formation at pH 2–3 include H-bonds, electrostatic, cation-π and hydrophobic interactions, and possibly some coordination complexes. How are these affected as plaques acclimate to the seawater pH of 8? Plaque adhesion and solidification are widely assumed to depend on seawater-actuated chemistry; however, experimental evidence on this point has been somewhat limited, even contradictory, so the data are worth scrutinizing.

Plaque interface

Predictions of pH-dependent changes in the interfacial coordination chemistry of catechol (Dopa) come from a variety of studies based on various techniques. Given their range and scope, these will be divided into catechol (Dopa)-based and Mfp-based studies.

Catechol-based experiments

On metal oxides such as alumina (McBride and Wesselink, 1988), titania (Bahri et al., 2011; Vega-Arroyo et al., 2005) and iron oxide surfaces, catechol (Dopa) binding is pH dependent, progressing from bidentate H-bonding to bidentate-binuclear coordinative bonding (Fig. 6A); that is, two H-bonds per catechol at pH ~3, to one H-bond and one coordination bond at pH ~5, and finally to two

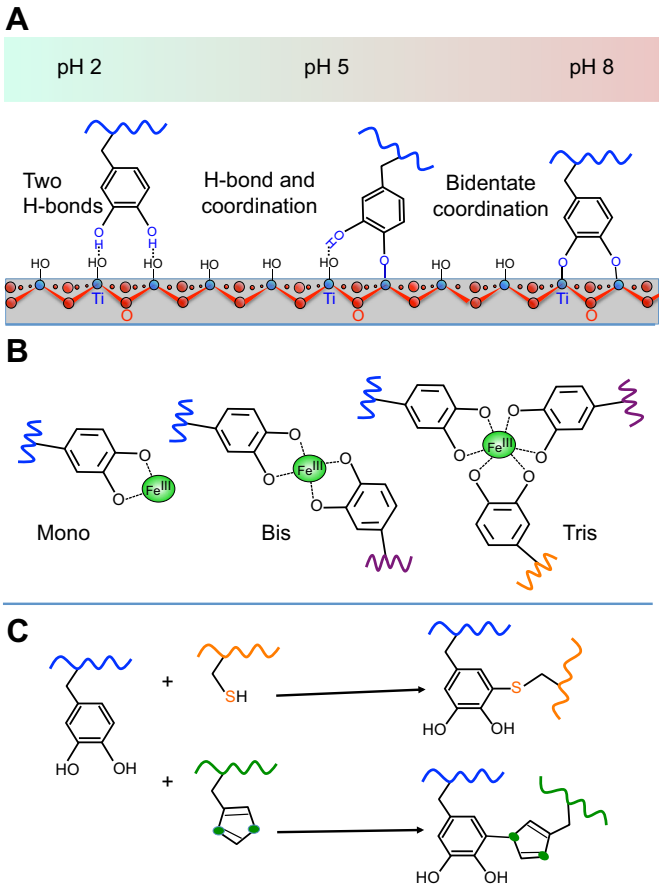

Fig. 6. Examples of plaque chemistry that change with pH. (A) Interfacial catechol bonding to metal oxide surfaces changes from H-bonds at acid pH to bidentate coordination at seawater pH. (B) Metal coordination by catechol (Dopa) increases in valency from none or one (no cross-linking) at acid pH to three at pH ~8.0 (cross-linking). (C) Covalent cross-links (Yu et al., 2013a,b; Holten-Andersen et al., 2011). These are formed after the catechols are oxidized to quinones in a pH-dependent enzyme-catalyzed reaction (optimum pH 8). The blue, green, orange and purple squiggles denote different protein chains. The reactions shown are not the only pH-sensitive changes taking place.

coordination bonds at pH ~8 (Li et al., 2010; Bahri et al., 2011; Mian et al., 2014). At pH 7–8, Dopa coordination to titania has a bond energy of 100 kJ/mol, which is approximately half as strong as a covalent bond and 5–10 times stronger than H-bonding at pH 7.5 (Lee et al., 2006). Adhesion critically depends on both hydroxyl groups of Dopa, with a breaking force five times greater than for a tethered monohydroxy tyrosine (Lee et al., 2006). Surface coordination probably goes beyond Dopa: other Mfp ligands such as imidazoles (histidine) also coordinate metal ions (Schmitt et al., 2000; Degtyar et al., 2014), but, according to the latest studies, these are largely cohesive interactions in plaques.

Mfp-based experiments

Dopa-containing Mfps like Mfp-3 and Mfp-5 are not accurately represented by simple catechols, thus experiments need to confirm catechol-mediated interactions using actual protein. Dopa residues in Mfp-3 and Mfp-1 form coordination complexes with titania surfaces at pH 5 and above (Yu et al., 2013a,b; Hwang et al., 2012), and synthetic Mfp-3 is coordinated to titania with Dopa, but not without Dopa. Moreover, a recombinant Mfp-5 fusion protein construct achieved up to six times more adhesion to titania, silica,

gold and polystyrene surfaces with Dopa than without (Zhong et al., 2014). Dopa coordination to surface metal oxides is not an option on all surfaces, but adhesion or adsorption will not necessarily be weaker without it. For instance, Dopa in Mfp-3 does not coordinate to calcium in HAP, however, adsorption to HAP is as extensive and resistant to desorption as adsorption to titania (Wei et al., 2016).

Interfacial catechol coordination chemistry is undeniably pH dependent, but what of the other possible surface interactions, such as H-bonds? In cases where H-bonding is charge mediated, e.g. between oppositely charged carboxylic acid and amine functional groups, the strongest interaction occurs at pH values above the acid pK_a and below the base pK_a (Valtiner et al., 2012). A shift, for example, from pH 3 to 8 would maximize negative charge on carboxylates (pK_a 4–5), and hence increase attraction to charged amines, which, with a typical pK_a of 10.4, would remain largely unchanged. However, the greater Debye screening (see Glossary) at the ionic strength (~0.7 M) of seawater would make the overall contribution of electrostatic interactions difficult to predict. For H-bonds that do not involve ionization, the impact of the dielectric constant (see Glossary) of the medium on interaction energy has yet to be determined (Israelachvili, 2011). Another electrostatic trend is predictable: electrostatic interactions between phosphate groups and surface cations become less soluble (i.e. less hydrated, more ionic) with pH increase to 8 (Shao and Stewart, 2010; Stayton et al., 2003) – this is the basis of anticorrosive coatings technology (Mequanint et al., 2003).

Plaque cohesion in seawater

Cohesion is also expected to change with exposure to seawater pH. Some of the H-bonds, cation-π and electrostatic interactions, and coordination complexes that exist between Mfps at acidic pH are different at pH 8. In particular, the H-bonds between Dopa residues are surprisingly robust and can, in the absence of oxidation, maintain noncovalent cohesion across a range of pH (Ahn et al., 2014). With >15 mol% lysine and Dopa in many Mfps, cation-π interactions are well-supported as participants in Mfp–Mfp cohesion (Lu et al., 2013a), but these are unlikely to change significantly between pH 2 and pH 8. As in adhesion, electrostatic interactions are weak at pH 2–3, but their strength probably increases as the increase to pH 8 ionizes more acidic groups without substantially reducing the charged amines (pK_a 10.4). One noteworthy electrostatic interaction in the context of pH is that between phosphate groups and Ca^{2+}/Mg^{2+}; these are ionic salts [the solubility product (see Glossary; K_{sp})=1×10^{-7} at 25°C] with solubility that decreases with increasing pH. Indeed, seawater pH has been used as an environmental cue to harden a synthetic coacervate based on *Phragmatopoma* cement (Shao and Stewart, 2010) and is likely to exert similar effects on mussel adhesives.

Mussels rely heavily on coordination chemistry for cohesion throughout the byssus. These coordination complexes are particularly interesting because they can be switched on and off by pH and consist of two types: imidazolato (histidine)–metal ion (Degtyar et al., 2014; Fullenkamp et al., 2013) and catecholato (Dopa)–iron complexes (Harrington et al., 2010; Hwang et al., 2010a; Zeng et al., 2010). Dopa–Fe coordination complexes hold Mfp-1 together in the SFA and in the byssal cuticle (Zeng et al., 2010; Harrington et al., 2010). The catecholate–iron complex of byssal cuticle (Fig. 6B) has three distinct pH-dependent steps known as mono, bis and tris that have been simulated (Xu, 2013); these refer to the ligand:metal stoichiometry (Taylor et al., 1996). The mono-Fe^{3+} form predominates at acidic pH, and cross-linking bis and tris forms with Fe^{3+} typically require pH >7, although the precise pH at which Dopa transitions from mono to bis to tris depends on the pK_a of the phenolic hydroxyls (Menyo et al., 2013; Taylor et al., 1996); in Dopa-proteins, this is likely to depend on local sequence. The neutral imidazole of histidine provides a suitable ligand for coordinative pH-dependent cross-linking and, in preCOLs, is typically associated with Cu^{2+} or Zn^{2+} ions (Harrington and Waite, 2007; Schmitt et al., 2015). The relative strength of binding depends, as with Dopa, on local environments (Degtyar et al., 2014). Each imidazolyl is monodentate and imidazoles of three to four His can coordinate Zn^{2+} in a square planar geometry; however, imidazolium (pK_a 6.5) has little to no tendency to bind metal below pH 6. The nanomechanical interaction between imidazole and Cu^{2+}, for example, is much weaker than that between Dopa and Fe^{3+} or Ti^{4+} (Schmitt et al., 2000), but histidine has the advantage of being less prone to oxidation.

The final cohesive interaction with a connection to ambient pH is covalent cross-linking associated with the oxidation of Dopa, which increases with pH (Fig. 6C). Covalent cross-linking partners for Dopa-quinone are quite diverse and include Dopa, Cys, His and Lys (Miserez et al., 2010; McDowell et al., 1999; Zhao and Waite, 2006). Covalent cross-links are known to form between symmetric films of oxidized Mfp-5, which require a high breaking force after setting for 12 h, although the long cross-linking time detracts from its biological relevance (Danner et al., 2012). Despite the spontaneity of Dopa oxidation to Dopa-quinone at seawater pH, mussels add an enzyme catalyst known as catechol-oxidase to byssal threads during thread production. Catechol-oxidase activity with a pH optimum of 8 is extractable from byssus (Waite, 1984), and catechol-oxidase-like protein sequences are present and abundant in the mussel foot transcriptome (Guerette et al., 2013). The role of this enzyme remains one of the least explored aspects of mussel byssus biochemistry.

Adhesion reconciled with biology and chemistry

Initial attempts to recapitulate seawater-actuated plaque adhesion with purified Mfps on mica surfaces failed, but were revealing nonetheless. At pH 2–3, where Cys and Dopa remain reduced (Nicklisch and Waite, 2012), Mfp-3 and Mfp-5 show repeatable high adhesion after many approach-and-separation cycles. However, as pH was increased in the asymmetric configuration under nonreducing conditions in the SFA, adhesion exhibited >90% losses (Fig. 3B). Why didn't adhesion increase as predicted? The explanation is surprisingly simple: mussels do not rely on single proteins for adhesion. At higher pH, those Dopa residues in Mfp-3 that are wrenched free from one of the mica surfaces during separation increasingly become oxidized to Dopa-quinone, and thus contribute little to surface H-bonds or coordination in the next adhesion cycle (Fig. 2F-ii′), except when rescued by antioxidants, particularly Mfp-6 (Yu et al., 2011b). Although Dopa-quinone could contribute to cohesion by cross-link formation, this would not be evident in the adhesion of asymmetric Mfp monolayers.

Oxidation of Dopa to quinone would reduce opportunities for coordination chemistry, but not every surface has coordination sites. If bidentate H-bonding is the only possible interaction with a given surface, does adhesion increase or decrease with increasing pH? This was tested on mica by protecting Dopa in Mfp-5 against oxidation at pH 7–8 by moderate complexation with borate (Kan et al., 2014). Adhesion of borate-protected Mfp-5 to mica at pH 3 and pH 8 remained about the same. AFM studies of single tethered Dopa binding to titania also support the idea that reduced Dopa, not Dopa-quinone, is strongly bound and this binding is completely reversible (Lee et al., 2006). Quinones provide opportunities for

Journal of Experimental Biology

Journal of Experimental Biology (2017) 220, 517-530 doi:10.1242/jeb.134056

adhesion to amine-functionalized (e.g. protein) surfaces, where the force to break (~2 nN) is consistent with formation of a covalent interfacial quinone–amine adduct (Lee et al., 2006; Utzig et al., 2016). Such adducts, however, are unlikely to form in the highly reducing environment of the plaque interface.

The interplay of chemistry and mechanics

Mussel byssal plaques undergo cyclic deformation during wave-associated lift and drag, perhaps thousands of times per day. Thus, it is tempting to ask whether the durability of the byssus derives from some specific structure–function relationships: can plaque chemistry explain why plaque fracture energy is 10^4 times greater than the adhesion energy of the most adhesive protein? A common way to improve toughness in a material is to increase its deformability, particularly its reversible deformability. According to Desmond et al. (2015), one type of extensive plaque deformation was shown to occur by partial delamination at the interface and yield with further extension within the bulk of the plaque. What happens when the interactions present in the deforming material are repeatedly disrupted by drag and lift forces?

It is instructive to predict the likely chemical changes during interfacial and cohesive deformation. Consider first an unloaded

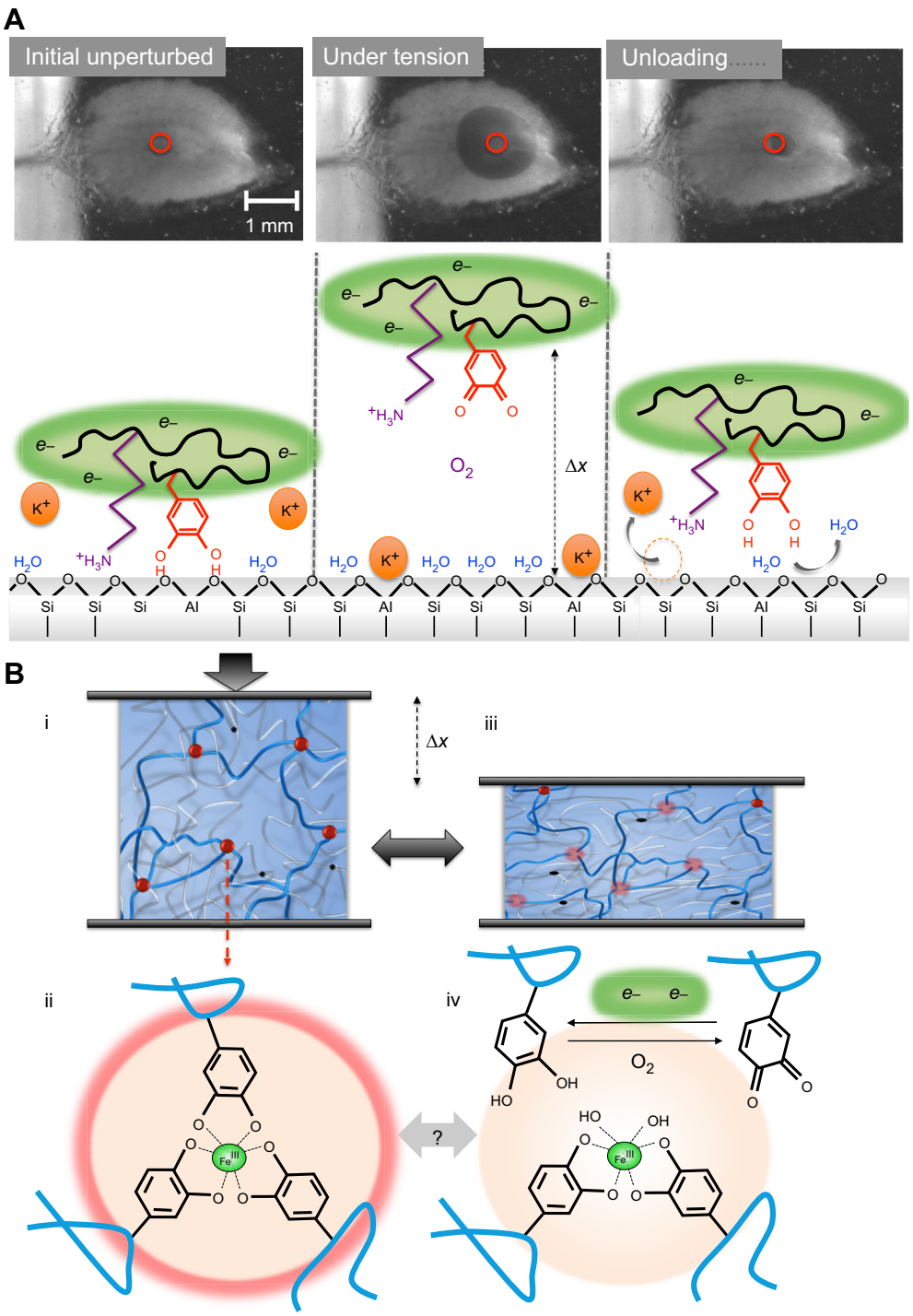

Fig. 7. Model of chemical adaptations during cyclic loading of the plaque. (A) Interfacial events as viewed from below using transparent mica. Initial unperturbed: the interface is intact, the substratum is dry, hydrated cations (K^+) are desorbed, Dopa is engaged by bidentate H- or coordination bonding, and the local environment is strongly reducing (green, e^-). Under tension: upon loading, bidentate Dopa and other interactions are debonded from the surface, the interface is displaced from the substrate by some distance Δx and the surface is reinvaded by O_2, salt and H_2O. Oxidation of Dopa (shown) and/or thiols follows and is repaired by the reducing e^- reservoir. Unloading: upon unloading, material relaxes, cations are evicted and the surface is dehydrated by Dopa, which rebonds to bidentate sites as under initial conditions. (B) Cohesive events. (i) The scheme of a double polymer network such as that in the byssal cuticle or plaque. The red balls denote tris-catecholato–iron cross-linking sites (ii) that unite three stiff (blue) Mfp-1 chains, for example. The black dots are covalent cross-linking sites that unite two compliant (silver) chains. (iii) During tensile or compressive deformation (gray arrows) by Δx (shown in compression), the tris links are at least partially disrupted (pale pink balls) allowing load transfer from stiff blue chains to compliant silver chains (iv). During disruption, catechols (Dopa) become prone to oxidation. Self-healing depends on the repair of oxidative damage. Dopa-quinone could go on to become covalent cross-links leading to embrittlement.

plaque interface (Fig. 7A): in the presence of either Mfp-5 or Mfp-3, the target surface will be desolvated (i.e. the water molecules will be displaced) and evicted of hydrated cations. Probable interfacial interactions involve bidentate H-bonds and/or bidentate coordination complexes between Dopa in Mfp-3 or Mfp-5 and metal oxides in the target surface in a reducing environment imposed by an abundance of Mfp-6. An applied load leads to de-adhesion in the center of the plaque; this region expands by peeling towards the edges and creates a strain Δx in the material (Fig. 7A). De-adhesion wrests Dopa groups from the surface, salt and water molecules return to create hydroxy–metal surfaces, and O_2 diffuses in. Disengaged, Dopa becomes vulnerable to oxidation, but because the plaque interface remains reducing for many weeks (Miller et al., 2015), Dopa losses to Dopa-quinone during interfacial failure may be mitigated in three ways: (1) cysteine thiols in Mfp-6 can eliminate O_2 by reducing it to water; (2) Dopa-quinone can be reduced back to Dopa by thiols; (3) Dopa-quinone can self-reduce (if a Lewis base is present) to the catechol moiety by forming Δ-dehydroDopa. In this way, when the plaque is unloaded and the interface is restored, the catechol-mediated desolvation and coordination of hydrated surface metal oxides can return. Importantly, this scenario enables material deformation and reversible yield, which are both critical toughening factors.

Catechol-based cohesive chemistry during deformation follows a similar trend: tris-catecholato–Fe^{3+} cross-links assumed to be intermolecular between Mfp-1 and Mfp-2 molecules have been detected in mature byssal cuticle as well as in the plaque core (Harrington et al., 2010; Hwang et al., 2011), where a double network of covalently and coordinatively cross-linked proteins exists. Fig. 7B assumes that the coordinative network is stiffer than the covalent one. As deformation proceeds, coordination complexes are broken to form a bis-catecholate–Fe^{3+} complex and free Dopa (Xu, 2013), which is prone to oxidation when uncomplexed (Das et al., 2015). Dopa-quinone is a poorer ligand than Dopa for iron complexation (Lee et al., 2006). However, the reducing environment, depending on its reducing capacity, again regenerates Dopa that is capable of recomplexing the Fe^{3+}, which is a necessary step for self-healing. Thread and plaque appear to have diversified their sacrificial coordination chemistry, in that a back-up of alternative oxidation-resistant ligands (e.g. imidazoles) and metals are complexed (Fig. 6B). Like the catecholate–Fe^{3+} complexes, these are also reversible, but their bond energies are significantly lower.

The emerging picture is fascinating but perplexing, because the mussel's reliance on Dopa for adaptable adhesion comes with a cost: getting the best interfacial and cohesive performance out of Dopa requires surface acidification, a substantial reducing reservoir and an uncanny ability to differentially control the redox of spatially and functionally distinct microenvironments. In mussels, the reducing reservoir appears to be based on Mfp-6, but how is this insulated against seawater? Future research should aim to identify the compliant covalent network in cohesion, and determine how the interplay between catechol–metal versus imidazole–metal coordination chemistry is tuned (Degtyar et al., 2014). The emerging picture also needs adjustment in one critical detail: seawater pH is decreasing globally. If actuation of mature byssal chemistry is tightly coupled with pH 8, and the pH of ambient seawater continues to decrease, then mussel byssus of the future may only achieve a fraction of its potential tenacity. This trend has already been reported for mussels in the Pacific Northwest (O'Donnell et al., 2013).

Conclusion

Mussel byssus formation is a tightly coupled choreography of chemistry and processing steps. Even though much remains unknown, a careful dissection of current knowledge inspires amazement at the intricacy and number of steps involved. For plaque formation, for example, the requirements include the acidic deposition of adhesive proteins, the highly reducing interfacial environment, the complex fluids (coacervates) used to concentrate, adsorb and invert protein phases, and pH ramps to increase ligand valency in metal coordination. As many of these steps appear to be adaptations to accommodate and regulate the reactivity of Dopa, one must ask why any organism would rely on an adhesive with such high management costs. Other organisms such as barnacles and sea stars have evolved perfectly good Dopa-less adhesives (Kamino, 2013; Hennebert et al., 2014). Perhaps investment in Dopa is related to its versatility, e.g. its capacity to multitask in removing surface hydration on mineral surfaces, tuning the redox environment, adsorbing to surfaces, controlling protein conformation, chelating metals and providing covalent cross-linking.

Whatever the mysterious appeal of Dopa to sessile organisms, the message to biotechnology is clear: do not mess with Dopa unless, like the mussel, you are prepared to micromanage pH and redox. The importance of redox for balancing the adhesion and cohesion of mussel mimetic adhesive polypeptides has been recognized for many years (e.g. Yu and Deming, 1998), but countermeasures to regulate the reactivity of catechol-functionalized synthetic polymers have only recently taken hold (Menyo et al., 2013; Holten-Andersen et al., 2011; Heo et al., 2012; Krogsgaard et al., 2015; Sedó et al., 2012). Understanding how a reducing interface is sustained between the plaque and substratum will be key to developing the best technologies. In many respects, the mussel dependence on Mfp-6 resembles the reliance of living cells on thioredoxins to maintain their internal redox poise (Banerjee, 2012), but how this is achieved without the benefit of cellular enzymes to recycle reducing poise in the mussel system eludes imagination (Nicklisch et al., 2016; Miller et al., 2015).

A second, equally important emerging theme is that chemistry isn't everything. Although biomimetic efforts to reproduce mussel adhesion began with co-opting Dopa or catechol functionalization for a variety of synthetic backbones (Sedó et al., 2012), they should not remain fixed there. Integrating chemical insights with higher length scale structure and architecture as well as time scales is likely to provide the best opportunities for improved adhesion technology. So far, there are few initiatives in this direction (Barrett et al, 2012; Menyo et al., 2015; Zhao et al., 2016).

Acknowledgements

The author particularly thanks J. Israelachvili and research associates, E. Danner, D. DeMartini, E. Filippidi, D. R. Miller, W. Wei, and J. Yu, for their many insights.

Competing interests

The author declares no competing or financial interests.

Funding

Grants from the National Science Foundation (Materials Research Science and Engineering Centers DMR 1121053) and the National Institutes of Health (R01 DE 018468) and generous gifts from the Lam Research Foundation and the Valois Family supported the wide-ranging research described. Deposited in PMC for release after 12 months.

References

Ahn, B. K., Lee, D. W., Israelachvili, J. N. and Waite, J. H. (2014). Surface-initiated self-healing of polymers in aqueous media. *Nat. Mater.* **13**, 867-872.

Allen, J. A., Cook, M., Jackson, D. J., Preston, S. and Worth, E. M. (1976). Observations on the rate of production and mechanical properties of the byssus threads of *Mytilus edulis*. *J. Mollusc. Stud.* **42**, 279-289.

Arnold, A. A., Byette, F., Séguin-Heine, M.-O., LeBlanc, A., Sleno, L., Tremblay, R., Pellerin, C. and Marcotte, I. (2012). Solid-State structure determination of

Journal of Experimental Biology

whole anchoring threads from the blue mussel *Mytilus edulis*. *Biomacromolecules* **14**, 132-141.
Ashby, M. F. (1983). The mechanical properties of cellular solids. *Metall. Trans.* **14A**, 1755-1769.
Ashton, N. N., Taggart, D. S. and Stewart, R. J. (2011). Silk tape nanostructure and silk gland anatomy of *Trichoptera*. *Biopolymers* **97**, 432-445.
Aumiller, W. M., Jr and Keating, C. D. (2016). Phosphorylation mediated RNA-peptide complex coacervation as a model for intracellular liquid organelles. *Nat. Chem.* **8**, 129-137.
Bahri, S., Jonsson, C. M., Jonsson, C. L., Azzollini, D., Sverjensky, D. M. and Hazen, R. M. (2011). Adsorption and surface complexation study of Dopa on Rutile (α-TiO_2) in NaCl solutions. *Environ. Sci. Technol.* **45**, 3959-3966.
Banerjee, R. (2012). Redox outside the box: linking extracellular redox remodeling with intracellular redox metabolism. *J. Biol. Chem.* **287**, 4397-4402.
Barrett, D. G., Fullenkamp, D. E., He, L., Holten Andersen, N., Lee, K. Y. C., Messersmith, P. B. (2012). pH-based regulation of hydrogel mechanical properties through mussel-inspired chemistry and processing. *Adv. Funct. Mater.* **23**, 1111-1119.
Bell, E. and Gosline, J. (1996). Mechanical design of mussel byssus: material yield enhances attachment strength. *J. Exp. Biol.* **199**, 1005-1017.
Bungenberg de Jong, H. G. (1949). Complex colloid systems. In *Colloid Science*, Vol. 2 (ed. H. R. Kruyt), pp. 335-432. Amsterdam: Elsevier Publishing Company, Inc.
Burkett, J. R., Wojtas, J. L., Cloud, J. L. and Wilker, J. J. (2009). A method for measuring adhesion strength of marine mussels. *J. Adhesion* **85**, 601-615.
Callow, J. A. and Callow, M. E. (2006). Biofilms. *Prog. Mol. Subcell. Biol.* **42**, 141-169.
Carrington, E. and Gosline, J. D. (2004). Mechanical design of mussel byssus: load cycle and strain rate dependence. *Am. Malacol. Bull.* **18**, 135-142.
Chollakup, R., Beck, J. B., Dirnberger, K., Tirrell, M. and Eisenbach, C. D. (2013). Polyelectrolyte molecular weight and salt effects on the phase behavior and coacervation of aqueous solutions of poly(acrylic acid) and poly(allyl)amine hydrochloride. *Macromolecules* **46**, 2376-2390.
Cooper, L. H. N. (1937). Oxidation-reduction potential of seawater. *J. Mar. Biol. Assoc. UK* **22**, 167-176.
Crisp, D. J., Walker, G., Young, G. A. and Yule, A. B. (1985). Adhesion and substrate choice in mussels and barnacles. *J. Colloid Interface Sci.* **104**, 40-50.
Danner, E. W., Kan, Y., Hammer, M. U., Israelachvili, J. N. and Waite, J. H. (2012). Adhesion of mussel foot protein mefp-5 to mica: and underwater superglue. *Biochemistry* **51**, 6511-6518. PMC 3428132.
Das, S., Miller, D. R., Kaufman, Y., Martinez Rodriguez, N. R., Pallaoro, A., Harrington, M. J., Gylys, M., Israelachvili, J. N. and Waite, J. H. (2015). Tough coating proteins: subtle sequence variation modulates cohesion. *Biomacromolecules* **16**, 1002-1008.
Degtyar, E., Harrington, M. J., Politi, Y. and Fratzl, P. (2014). The mechanical role of metal ions in biogenic protein-based materials. *Angew. Chem. Int. Ed. Engl.* **53**, 12024-12044.
Denny, M. W. and Gaylord, B. (2010). Marine ecomechanics. *Annu. Rev. Mar. Sci.* **2**, 89-114.
Desmond, K. W., Zacchia, N. A., Waite, J. H. and Valentine, M. T. (2015). Dynamics of mussel holdfast plaque detachment. *Soft Mat.* **11**, 6832-6839.
Dougherty, D. A. (2013). The cation-π interaction. *Acc. Chem Res.* **46**, 885-893.
Filippidi, E., DeMartini, D., de Molina, P. M., Danner, E. W., Kim, J., Helgeson, M. E., Waite, J. H. and Valentine, M. T. (2015). The microscopic network structure of mussel (*Mytilus*) adhesive plaques. *J. R. Soc. Interface* **12**, 20150614.
Fullenkamp, D. E., He, L., Barrett, D. G., Burghardt, W. R. and Messersmith, P. B. (2013). Mussel-inspired histidine-based transient network metal coordination hydrogels. *Macromolecules* **46**, 1167-1174.
Guerette, P. A., Hoon, S., Seow, Y., Raida, M., Masic, A., Wong, F. T., Ho, V. H. B., Kong, K. W., Demiral, M. C., Pena-Francesch, A. et al. (2013). Accelerating the design of biomimetic materials by integrating RNA-seq with proteomics and materials science. *Nat. Biotechnol.* **31**, 908-915.
Guzman, N. A., Fuller, G. C. and Dixon, J. E. (1990). Hydroxyproline containing proteins and their hydroxylations by genetically distinct prolyl-4-hydroxylases. In *Organization and Assembly of Plant and Animal Extracellular Matrix* (ed. W. S. Adair and R. P. Mecham), pp. 302-346. San Diego, CA: Academic Press, Inc.
Harrington, M. J. and Waite, J. H. (2007). Holdfast heroics: comparing the molecular and mechanical properties of *Mytilus californianus* byssal threads. *J. Exp. Biol.* **210**, 4307-4318.
Harrington, M. J., Masic, A., Holten-Andersen, N., Waite, J. H. and Fratzl, P. (2010). Iron-clad fibers: a metal-based biological strategy for hard flexible coatings. *Science* **328**, 216-220. PMC 3087814.
Hassenkam, T., Gutsmann, T., Hansma, P., Sagert, J. and Waite, J. H. (2004). Giant bent-core mesogens in the thread forming process of marine mussels. *Biomacromolecules* **5**, 1351-1355.
Helm, C. A., Knoll, W. and Israelachvili, J. N. (1991). Measurement of ligand-receptor interactions. *Proc. Nat. Acad. Sci. USA* **88**, 8169-8173.
Hennebert, E., Wattiez, R., Demeuldre, M., Ladurner, P., Hwang, D. S., Waite, J. H. and Flammang, P. (2014). Sea star tenacity mediated by a protein that fragments, then aggregates. *Proc. Nat. Acad. Sci. USA* **111**, 6317-6322.
Heo, J., Kang, T., Jang, S. G., Hwang, D. S., Spruell, J. M., Killops, K. L., Waite, J. H. and Hawker, C. J. (2012). Improved performance of protected catecholic polysiloxanes for bio-inspired wet adhesion to surface oxides. *J. Am. Chem. Soc.* **134**, 20139-20145.
Holten-Andersen, N., Fantner, G. E., Hohlbauch, S., Waite, J. H. and Zok, F. W. (2007). Protective coatings on extensible biofibres. *Nat. Mater.* **6**, 669-672.
Holten-Andersen, N., Lee, B. P., Messersmith, P. B., Lee, K. Y. C. and Waite, J. H. (2011). pH-induced mussel metal-ligand crosslinks yield self-healing polymer networks with near-covalent elastic moduli. *Proc. Nat. Acad. Sci. USA* **108**, 2651-2655.
Hurlburt, C. G. and Hurlburt, S. W. (1975). Blue gold: mariculture of the edible blue mussel. *Mar. Fish. Rev.* **37**, 11-18.
Hutchinson, N., Nagarkar, S., Aitchison, J. C. and Williams, G. A. (2006). Microspatial variation in marine biofilm abundance on intertidal rock surfaces. *Aquat. Microbiol. Ecol.* **42**, 187-197.
Hwang, D. S. and Waite, J. H. (2012). Three intrinsically unstructured mussel adhesive proteins, Mfp-1, Mfp-2 and Mfp-3: analysis by circular dichroism. *Protein Sci.* **21**, 1689-1695.
Hwang, D. S., Zeng, H., Masic, A., Harrington, M. J., Israelachvili, J. N. and Waite, J. H. (2010a). Fe^{3+}-dependent cohesion of a prominent protein of mussel adhesive plaques. *J. Biol. Chem.* **285**, 25850-25858. PMC 2919147.
Hwang, D. S., Zeng, H., Srivastava, A., Krogstad, D. V., Tirrell, M., Israelachvili, J. N. and Waite, J. H. (2010b). Complex coacervation of a recombinant mussel adhesive protein and hyaluronic acid - viscous and interfacial properties. *Soft Mat.* **6**, 3232-3236. PMC 3085400.
Hwang, D. S., Harrington, M. J., Lu, Q., Masic, A., Zeng, H. and Waite, J. H. (2012). Mussel foot protein-1 interaction with titania surfaces. *J. Mater. Chem.* **22**, 15530-15533.
Inoue, K., Takeuchi, Y., Miki, D., Odo, S., Harayama, S. and Waite, J. H. (1996). Cloning, sequencing and sites of expression of genes for the hydroxyarginine-containing adhesive-plaque protein of the mussel *Mytilus galloprovincialis*. *Eur. J. Biochem.* **239**, 172-176.
Israelachvili, J. N. (2011). *Intermolecular and Surface Forces*, pp. 274. Amsterdam, NL: Academic Press.
Kamino, K. (2013). Minireview: barnacle adhesives and adhesion. *Biofouling* **29**, 735-749.
Kan, Y., Danner, E. W., Israelachvili, J. N., Chen, Y. and Waite, J. H. (2014). Boronate complex formation with Dopa containing mussel adhesive protein retards pH-induced oxidation and enables adhesion to mica. *PLOS ONE* **9**, e.0108869.
Kier, W. M. and Smith, A. M. (2002). The structure and adhesive mechanism of octopus suckers. *Integr. Comp. Biol.* **42**, 1146-1153.
Kim, S., Huang, J., Lee, Y., Dutta, S., Yoo, H. Y., Jung, Y. M., Jho, Y. S., Zeng, H. and Hwang, D. S. (2016). Complexation and coacervation of like-charged polyelectrolytes inspired by mussels. *Proc. Nat. Acad. Sci. USA* **113**, E847-E853.
Koide, M., Lee, D. S. and Goldberg, E. D. (1982). Metal and transuranic records in mussel shells, byssal threads and tissues. *Estuar. Coast Shelf Sci.* **15**, 679-695.
Krogsgaard, M., Nue, V. and Birkedal, H. (2015). Mussel-inspired materials: self-healing through coordination chemistry. *Chem. Eur. J.* **22**, 844-957.
Lee, H., Scherer, N. F. and Messersmith, P. B. (2006). Single-molecule mechanics of mussel adhesion. *Proc. Nat. Acad. Sci. USA* **103**, 12999-13003.
Lee, B. P., Messersmith, P. B., Israelachvili, J. N. and Waite, J. H. (2011). Mussel inspired adhesives and coatings. *Annu Rev Mater. Res.* **41**, 99-132.
Li, S.-C., Chu, L.-N., Gong, X.-Q. and Diebold, U. (2010). Hydrogen bonding controls the dynamics of catechol adsorbed on a TiO_2 (110) surface. *Science* **328**, 882-884.
Loeb, G. I. and Neihof, R. A. (1975). Marine conditioning films. *Adv. Chem. Ser.* **145**, 319-335.
Lu, Q., Oh, D. X., Lee, Y., Jho, Y., Hwang, D. S. and Zeng, H. (2013a). Nanomechanics of cation-π interactions in aqueous solution. *Angew. Chem. Int. Ed.* **52**, 3944-3948.
Lu, Q., Danner, E., Waite, J. H., Israelachvili, J. N., Zeng, H. and Hwang, D. S. (2013b). Adhesion of mussel foot proteins to different substrate surfaces. *J. R. Soc. Interface* **10**, 20120759.
Maier, G. P., Rapp, M. V., Waite, J. H., Israelachvili, J. N. and Butler, A. (2015). Adaptive synergy between catechol and lysine promotes wet adhesion by surface salt displacement. *Science* **349**, 628-632.
Martinez Rodriguez, N. R., Das, S., Kaufman, Y., Israelachvili, J. N. and Waite, J. H. (2015). Interfacial pH during mussel adhesive plaque formation. *Biofouling* **31**, 221-227.
McBride, M. B. and Wesselink, L. G. (1988). Chemisorption of catechol on gibbsite, boehmite and noncrystalline alumina surfaces. *Environ. Sci. Technol.* **22**, 703-708.
McDowell, L. M., Burzio, L. A., Waite, J. H. and Schaefer, J. (1999). Rotational echo double resonance detection of crosslinks formed in mussel byssus under high flow stress. *J. Biol. Chem.* **274**, 20293-20295.
Menyo, M., Hawker, C. J. and Waite, J. H. (2013). Versatile tuning of supramolecular hydrogels through metal complexation of oxidation resistant catechol inspired ligands. *Soft Mat.* **9**, 10314-10323.

Menyo, M., Hawker, C. R. and Waite, J. H. (2015). Strain-dependent stiffness and recovery in inter-penetrating network hydrogels through sacrificial metal coordination bonds. *ACS Macro Lett.* **4**, 1200-1204.
Mequanint, K., Sanderson, R. and Pasch, H. (2003). Adhesion properties of phosphate- and siloxane-containing polyurethane dispersions to steel: an analysis of the metal-coating interface. *J. Appl. Polym. Sci.* **88**, 900-907.
Mian, S. A., Yang, L.-M., Saha, L. C., Ahmed, E., Ajmal, M. and Ganz, E. (2014). A fundamental understanding of catechol and water adsorption on a hydrophilic silica surface: exploring the underwater adhesion mechanism of mussels on an atomic scale. *Langmuir* **30**, 6906-6914.
Miki, D., Takeuchi, Y., Inoue, K. and Odo, S. (1996). Expression sites of two byssal protein genes of *Mytilus galloprovincialis*. *Biol. Bull.* **190**, 213-217.
Miller, D. R., Spahn, J. E. and Waite, J. H. (2015). The staying power of adhesion-associated antioxidant activity in *Mytilus californianus*. *J. R. Soc. Interface* **12**, 20150614.
Mirshafian, R., Wei, W., Israelachvili, J. N. and Waite, J. H. (2016). α,β-Dehydro-Dopa: a hidden participant in mussel adhesion. *Biochemistry* **55**, 743-750.
Miserez, A., Rubin, D. J. and Waite, J. H. (2010). Cross-linking chemistry of squid beak. *J. Biol. Chem.* **285**, 38115-38124.
Nicklisch, S. C. T. and Waite, J. H. (2012). Role of redox in Dopa-mediated marine adhesion. *Biofouling* **28**, 865-877.
Nicklisch, S. C. T., Spahn, J. E., Zhou, H., Gruian, C. M. and Waite, J. H. (2016). The redox capacity of an extracellular matrix protein associated with adhesion in *Mytilus californianus*. *Biochemistry* **55**, 2022-2030.
O'Donnell, M. J., George, M. N. and Carrington, E. (2013). Mussel byssus attachment weakened by ocean acidification. *Nat. Clim. Change* **3**, 587-590.
Olivieri, M. P., Wollman, R. M. and Alderfer, J. L. (1997). Nuclear magnetic resonance spectroscopy of mussel adhesive protein repeating peptide segment. *J. Peptide Res.* **50**, 436-442.
Petrone, L., Kumar, A., Sutanto, C. N., Patil, N. J., Kannan, S., Palaniappan, A., Amini, S., Zappone, B., Verma, C. and Miserez, A. (2015). Mussel adhesion is dictated by time-regulated secretion and molecular conformation of mussel adhesive proteins. *Nat. Commun.* **6**, 8737.
Qin, Z. and Buehler, M. J. (2013). Impact tolerance in mussel thread networks by heterogeous material distribution. *Nat. Commun.* **4**, 2187 (electronic).
Qin, X. and Waite, J. H. (2001). Polyphosphoprotein from the adhesive pads of *Mytilus edulis*. *Biochemistry* **40**, 2887-2893.
Ricciardi, A. (1998). Global range expansion of the Asian mussel *Limnoperna fortunei* (Mytilidae): another fouling threat to freshwater systems. *Biofouling* **13**, 97-106.
Rzepecki, L. M., Nagafuchi, T. and Waite, J. H. (1991). α, β-Dehydro-3,4-dihydroxyphenylalanine derivatives: potential schlerotization intermediates in natural composite materials. *Arch. Biochem. Biophys.* **285**, 17-26.
Sagert, J. and Waite, J. H. (2009). Hyperunstable matrix proteins in the byssus of *Mytilus galloprovincialis*. *J. Exp. Biol.* **212**, 2224-2236.
Schmitt, L., Ludwig, M., Gaub, H. and Tampe, R. (2000). A metal-chelating microscopy tip as a new toolbox for single-molecule experiments by atomic force microscopy. *Biophys. J.* **78**, 3275-3285.
Schmitt, C. N. Z., Politi, Y., Reinecke, A. and Harrington, M. J. (2015). Role of sacrificial protein-metal bond exchange in mussel byssal thread self-healing. *Biomacromolecules* **16**, 2852-2861.
Schneider, R. P. (1996). Conditioning film induced modification of substratum physicochemistry–analysis by contact angles. *J. Colloid Interf. Sci.* **182**, 204-213.
Sedó, J., Saiz-Poeu, J., Busque, F. and Ruiz-Molina, D. (2012). Catechol-based biomimetic functional materials. *Adv. Mater.* **25**, 653-701.
Shao, H. and Stewart, R. J. (2010). Biomimetic underwater adhesives with environmentally triggered setting mechanisms. *Adv. Mater.* **22**, 729-733.
Shin, J. M., Munson, K., Vagin, O. and Sachs, G. (2009). The gastric HK-ATPase: structure, function and inhibition. *Pflugers Arch.* **457**, 609-622.
Smith, A. M. (1991). The role of suction in the adhesion of limpets. *J. Exp. Biol.* **161**, 151-169.
Spuskanyuk, A. V., McMeeking, R. M., Deshpande, V. S. and Arzt, E. (2008). The effect of shape on the adhesion of fibrillar surfaces. *Acta Biomater.Acta Biomater.* **4**, 1669-1676.
Stayton, P. S., Drobny, G. P., Shaw, W. J., Long, J. R. and Gilbert, M. (2003). Structure and dynamics of hydrated statherin on hydroxyapatite as determined by solid-state NMR. *Crit. Rev. Oral Biol. Med.* **14**, 370-376.
Strathmann, H. and Kock, K. (1977). Formation mechanism of phase inversion membranes. *Desalination* **21**, 241-255.
Suhre, M. H., Gertz, M., Steegborn, C. and Scheibel, T. (2014). Structural and functional features of a collagen binding matrix protein from the mussel byssus. *Nat. Commun.* **5**, 3392.
Tamarin, A. and Keller, P. J. (1972). An ultrastructural study of the byssal thread forming system in Mytilus. *J. Ultrastructure Res.* **40**, 401-416.
Tamarin, A., Keller, P. J. and Askey, J. (1972). The structure and formation of byssus attachment plaque in Mytilus. *J. Morphology* **149**, 199-222.
Taylor, S. W., Chase, D. B., Emptage, M. H., Nelson, M. J. and Waite, J. H. (1996). Ferric ion complexes of a Dopa-containing adhesive protein from *Mytilus edulis*. *Inorg. Chem.* **35**, 7572-7577.
Taylor, S. W., Kammerer, B. and Bayer, E. (1997). New perspectives in the chemistry and biochemistry of the tunichromes and related compounds. *Chem. Rev.* **97**, 333-346.
Thompson, T. E. (1983). Detection of epithelial acid secretions in marine molluscs: review of techniques, and new analytical methods. *Comp. Biochem. Physiol.* **74A**, 615-621.
Utzig, T., Stock, P. and Valtiner, M. (2016). Resolving nonspecific and specific adhesive interactions of catechols at solid/liquid interfaces at the molecular scale. *Angew. Chem. Int Ed Engl.* **55**, 9524-9528.
Valtiner, M., Donaldson, S. H., Gebbie, M. A. and Israelachvili, J. N. (2012). Hydrophobic forces, electrostatic steering, and acid-base bridging between, smooth self-assembled monolayers and end-functionalized PEGolated lipid bilayers. *J. Am. Chem. Soc.* **134**, 1746-1753.
Vega-Arroyo, M., LeBreton, P. R., Rajh, T., Zapol, P. and Curtiss, L. A. (2005). Density functional study of the TiO_2-dopamine-complex. *Chem. Phys. Lett.* **406**, 306-311.
Vitellaro Zuccarello, L. (1980). The collagen gland of *Mytilus galloprovincialis*: An ultrastructural and cytochemical study on secretory granules. *J. Ultrastructure Res.* **73**, 135-147.
Waite, J. H. (1984). Catechol oxidase in the byssus of the common mussel. *J. Mar. Biol. Assoc. UK* **65**, 359-371.
Waite, J. H. (1992). Formation of the mussel byssus: anatomy of a natural manufacturing process. In *Results and Problems in Cell Differentiation*, vol. 19 (ed. S.T. Case) Biopolymers, pp. 27-54. Berlin: Springer.
Waite, J. H., Jensen, R. and Morse, D. E. (1992). Cement precursor proteins of the reef-building polychaete *Phragmatopoma californica* (Fewkes). *Biochemistry* **31**, 5733-5788.
Wake, W. C. (1982). *Adhesion and the Formulation of Adhesives*, pp. 189-199. London, UK: Applied Science Publishers.
Wei, W., Tan, Y., Martinez Rodriguez, N. R., Yu, J., Israelachvili, J. N. and Waite, J. H. (2013a). A mussel-derived one-component adhesive coacervate. *Acta Biomater.* **10**, 1663-1670.
Wei, W., Yu, J., Broomell, C. C., Israelachvili, J. N. and Waite, J. H. (2013b). Hydrophobic enhancement of Dopa-mediated adhesion in a mussel foot protein. *J. Am. Chem. Soc.* **135**, 377-383.
Wei, W., Yu, J., Gebbie, M., Tan, Y., Martinez, N. R., Israelachvili, J. N. and Waite, J. H. (2014). The bridging adhesion of mussel-inspired peptides: the role of charge, molecular weight and surface type. *Langmuir* **31**, 1105-1112.
Wei, W., Petrone, L., Tan, Y. P., Cai, H., Israelachvili, J. N., Miserez, A. and Waite, J. H. (2016). Underwater surface drying peptide inspired by a mussel adhesive protein. *Adv. Funct. Mater.* **26**, 3496-3507.
Witman, J. D. (1987). Subtidal coexistence: storms, grazing, mutualism, and the zonation of kelps and mussels. *Ecol. Monogr.* **57**, 167-187.
Xu, Z. (2013). Mechanics of metal-catecholate complexes: the roles of coordination state and metal types. *Sci. Rep.* **3**, 2914.
Yonge, C. M. (1962). On the primitive significance of the byssus in the bivalvia and its effects in evolution. *J. Mar. Biol. Assoc. UK* **42**, 113-125.
Yu, M. and Deming, T. J. (1998). Synthetic polypeptide mimics of marine adhesives. *Macromolecules* **31**, 4739-4745.
Yu, J., Wei, W., Danner, E., Israelachvili, J. and Waite, J. H. (2011a). Effects of interfacial redox in mussel adhesive protein films on mica. *Adv. Mater.* **23**, 2362-2366. PMC 3221558.
Yu, J., Wei, W., Danner, E., Ashley, R. K., Israelachvili, J. N. and Waite, J. H. (2011b). Mussel protein adhesion depends on interprotein thiol-mediated redox modulation. *Nat. Chem. Biol.* **7**, 588-590.
Yu, J., Kan, Y., Rapp, M., Danner, E., Wei, W., Das, S., Miller, D. R., Waite, J. H. and Israelachvili, J. N. (2013a). Adaptive hydrophobic and hydrophilic interactions of mussel foot proteins with organic thin films. *Proc Nat Acad Sci USA* **110**, 15680-15685.
Yu, J., Wei, W., Menyo, M. S., Masic, A., Waite, J. H. and Israelachvili, J. N. (2013b). Adhesion of mussel foot protein-3 to TiO_2 surfaces: the effect of pH. *Biomacromolecules* **14**, 1072-1077.
Zeng, H., Hwang, D. S., Israelachvili, J. N. and Waite, J. H. (2010). Strong reversible Fe^{3+}-mediated bridging between Dopa-containing protein films in water. *Proc. Nat. Acad. Sci. USA* **107**, 12850-12853. PMC 2919964.
Zhao, H. and Waite, J. H. (2006). Linking adhesive and structural proteins in the attachment plaque of *Mytilus californianus*. *J. Biol. Chem.* **281**, 26150-29158.
Zhao, H., Sun, C. J., Stewart, R. J. and Waite, J. H. (2005). Cement proteins of the tube-building polychaete *Phragmatopoma californica*. *J. Biol. Chem.* **280**, 42938-42944.
Zhao, Q., Lee, D. W., Ahn, B. K., Israelachvili, J. N. and Waite, J. H. (2016). Underwater contact adhesion and micro-architecture in polyelectrolyte complexes actuated by solvent exchange. *Nat. Mater.* **15**, 407-412.
Zhong, C., Gurry, T., Cheng, A. A., Downey, J., Deng, Z., Stultz, C. M. and Lu, T. K. (2014). Strong underwater adhesives made by self-assembling multi-protein nanofibres. *Nat. Nanotechnol.* **9**, 858-866.

Journal of Experimental Biology